

Qualitative properties of numerical methods for the inhomogeneous geometric Brownian motion

Irene Tubikanec*, Massimiliano Tamborrino†, Petr Lansky‡, Evelyn Buckwar*§

Abstract

We introduce the inhomogeneous geometric Brownian motion (IGBM) as a test equation for analysing qualitative features of numerical methods applied to multiplicative noise stochastic ordinary differential equations of Itô type with an inhomogeneous drift. The usual linear stability analysis of a constant equilibrium (in the mean-square or almost-sure sense) cannot be carried out for these equations as they do not have one. However, the conditional and asymptotic mean and variance of the IGBM are explicitly known and the process can be characterised according to Feller's boundary classification. We compare four splitting schemes, two based on the Lie-Trotter composition and two based on the Strang approach, with the frequently used Euler-Maruyama and Milstein methods. First, we derive closed-form expressions for the conditional and asymptotic means and variances of all considered numerical schemes and analyse the resulting errors with respect to the true quantities. In contrast to the frequently applied methods, the splitting schemes do not require extra conditions for the existence of the asymptotic moments and outperform them in terms of the variance. Second, we prove that the constructed splitting schemes preserve the boundary properties of the process, independently of the choice of the discretisation step, whereas the Euler-Maruyama and Milstein methods do not.

Keywords

Geometric Brownian motion, Inhomogeneous drift, Feller's boundary classification, Numerical splitting schemes, Boundary preservation, Moment preservation

AMS subject classifications

60H10, 60H35, 65C20, 65C30

Acknowledgements

This work was supported by the Austrian Exchange Service (OeAD), bilateral project CZ 19/2019 and by the Austrian Science Fund (FWF), W1214-N15, project DK 14.

1 Introduction

A large part of numerical analysis of differential or integral equations is devoted to convergence of numerical methods in a suitable sense. These are limit results for the stepsize in time and/or space going to zero over a finite interval and, of course, numerical methods which do not converge

*Institute for Stochastics, Johannes Kepler University Linz (irene.tubikanec@jku.at, evelyn.buckwar@jku.at)

†Department of Statistics, University of Warwick (massimiliano.tamborrino@warwick.ac.uk)

‡Institute of Physiology, Czech Academy of Sciences (lansky@biomed.cas.cz)

§Centre for Mathematical Sciences, Lund University

should not be used. Nevertheless, in practice, the simulation of a solution of the equation requires to fix a stepsize. In consequence, the numerical method can be viewed as a discrete dynamical system, which may or may not have the same properties and behaviour as the original problem. In the worst case, although the method converges, the discretisation step may alter the essential properties of the model, making the numerical method inefficient or practically useless. Therefore, the investigation of the qualitative properties of numerical methods constitutes a crucial part of numerical analysis.

Numerical analysis of stochastic differential equations (SDEs) is an important tool for understanding the properties of dynamical systems under the influence of noise. In recent years, this area has developed at a fast pace. In the field of stochastic numerical analysis, beyond convergence, linear stability analysis in the mean-square or almost sure sense has been introduced by Mitsui and Saito [44, 45], based on stability theory in the sense of Lyapunov [28]. Linear stability analysis for systems of SDEs has been discussed in [10, 13, 46, 50]. Nonlinear stability concepts, symplectic methods, Lie group methods, variational integrators, etc., known in the deterministic setting, have been carried over to the SDE case [24, 31, 34, 38]. The standard setting of linear stability analysis for SDEs requires equations with multiplicative noise and a deterministic constant equilibrium solution for which the drift and diffusion components become zero simultaneously. In this framework, the geometric Brownian motion (GBM) [5, 36] has often been used as a tractable test equation [12, 23, 45]. However, neither SDEs with additive noise nor SDEs with inhomogeneous drift are covered by this approach. In [11], the authors provide a review of methods proposed to cover the first case. Here, we contribute to the second case, introducing the inhomogeneous GBM (IGBM) [1, 18, 52], described by the Itô SDE

$$dY(t) = \left(-\frac{1}{\tau}Y(t) + \mu \right) dt + \sigma Y(t)dW(t), \quad t \geq 0, \quad Y(0) = Y_0, \quad \tau, \sigma > 0,$$

as a test equation. This process is characterised by the constant inhomogeneous term $\mu \in \mathbb{R}$ and coincides with the well-studied GBM for $\mu = 0$. The IGBM is commonly applied in mathematical finance, neuroscience and other fields. It is a member of the Pearson diffusion class [20] and also known as GBM with affine drift [32], geometric Ornstein-Uhlenbeck process [25], mean reverting GBM [47], Brennan-Schwarz model [9, 15], GARCH model [6] or as Lognormal diffusion with exogenous factors [22].

Differently from other well-known Pearson diffusions, such as the Ornstein-Uhlenbeck process [5, 30] and the square-root process [16, 17, 19, 30], the transition density of the IGBM does not have a practical closed-form expression [52] and an exact simulation scheme is not available. Our goal is to propose numerical solutions able to preserve qualitative features of the IGBM for a fixed time discretisation step, and to provide a comparative analysis of different methods. Besides analysing the commonly used Euler-Maruyama and Milstein schemes, we extend our discussion to four splitting schemes, two based on the Lie-Trotter composition and two on the Strang approach [49]. We refer to [7, 37] for an exhaustive discussion of splitting methods for broad classes of ordinary differential equations (ODEs) and to [2, 3, 8, 31, 38, 40, 41, 42, 48] for extensions to SDEs.

In the following, we introduce the properties of the IGBM, linking to the GBM. If $\mu = 0$, a unique constant solution (equilibrium), making both the drift and the diffusion coefficient vanish, exists, namely $Y(t) \equiv 0$ for $t \geq 0$. Conditioned on $Y_0 > 0$, the mean and variance of the GBM are given by $\mathbb{E}[Y(t)|Y_0] = Y_0 e^{-t/\tau}$ and $\text{Var}(Y(t)|Y_0) = Y_0^2 e^{-2t/\tau} (e^{\sigma^2 t} - 1)$. Consequently, the asymptotic mean is zero and the asymptotic variance is zero, if $\sigma^2 \tau < 2$. In terms of linear stochastic stability analysis, this means that the equilibrium solution is asymptotically first moment stable and asymptotically second moment stable, if $\sigma^2 \tau < 2$. The latter property is often referred to as asymptotic mean-square stability in the literature [5, 23, 45]. For the inhomogeneous equation, the stability theory of a constant equilibrium in the mean-square sense cannot be applied as the equation does not have one. However, the conditional and asymptotic mean and variance of the IGBM are explicitly known. Our first goal is to propose numerical solutions which accurately reproduce these quantities. In particular, we derive closed-form expressions for the conditional

and asymptotic means and variances of both the frequently applied Euler-Maruyama and Milstein schemes and the constructed splitting schemes. These quantities differ from the true ones. For this reason, we compare the resulting biases. Our results for the Euler-Maruyama and Milstein methods cover those for the well-studied GBM available in the literature.

Moreover, if $\mu = 0$, it is known that $\mathbb{P}(\lim_{t \rightarrow \infty} Y(t) = 0 | Y_0 > 0) = 1$, since $\tau > 0$. In terms of linear stochastic stability analysis, this means that the equilibrium solution is asymptotically almost sure stable. In the framework of Feller's boundary classification [27], this means that, given $Y_0 > 0$, the boundary zero is unattainable and attracting [39], i.e., the process cannot reach the boundary in finite time, but is attracted to it as time tends to infinity. For the inhomogeneous equation, the stability theory in the almost sure sense cannot be applied. However, depending on the parameter μ , the IGBM possesses different properties at the boundary zero, according to Feller's classification. Our second goal is to derive numerical solutions which preserve these boundary properties. This is particularly important, since the nature of a boundary may force the process to change its behaviour near or at the boundary. While frequently applied numerical methods may fail in preserving such properties [4, 7, 35, 41], we prove that all four derived splitting schemes preserve them. While Feller's boundary classification is a standard concept in the field of stochastic analysis, it is not so often adopted as a qualitative feature in stochastic numerics. An exception constitutes the topic of positivity preservation, often studied in terms of the square-root process [4, 26, 35, 40] and the domain-invariance [21, 33, 43]. For an investigation of these issues related to numerical splitting methods, we refer to [33, 40]. For a discussion of Feller's classification in the context of splitting schemes, we refer to [41], where the focus lies on proving convergence results and only Lie-Trotter compositions are considered.

The paper is organised as follows. In Section 2, we introduce the IGBM and recall its properties. In Section 3, we provide a brief account of the numerical splitting approach, describing the Lie-Trotter and the Strang compositions and deriving four different numerical solutions based on them. In Section 4, we provide closed-form expressions for the conditional and asymptotic means and variances of the investigated numerical solutions, analyse the resulting biases and discuss the boundary preservation. In Section 5, we illustrate the theoretical results of Section 4 through a series of numerical experiments. Moreover, we investigate the ability of the derived schemes to approximate the underlying stationary distribution and study their behaviour at the lower boundary. Conclusions are reported in Section 6.

2 The IGBM and its properties

The IGBM is described by the Itô SDE

$$dY(t) = \underbrace{\left(-\frac{1}{\tau}Y(t) + \mu\right)dt}_{:=F(Y(t))} + \underbrace{\sigma Y(t)}_{:=G(Y(t))} dW(t), \quad t \geq 0, \quad Y(0) = Y_0, \quad (1)$$

where $\tau, \sigma > 0$, $\mu \in \mathbb{R}$ and $W = (W(t))_{t \geq 0}$ is a standard Wiener process defined on the probability space $(\Omega, \mathcal{F}, \mathbb{P})$ with a filtration $\mathcal{F} = (\mathcal{F}(t))_{t \geq 0}$ generated by W . The initial value Y_0 is either a deterministic non-negative constant or an $\mathcal{F}(0)$ -measurable non-negative random variable with finite second moment. Since (1) is a linear and autonomous SDE, a unique strong solution process $Y = (Y(t))_{t \geq 0}$ exists [5, 36]. The solution of the homogeneous SDE (if $\mu = 0$) corresponds to the well-known GBM. Applying the variation of constants formula [36] to (1), which represents its unique solution in terms of the embedded GBM, yields

$$Y(t) = e^{-(\frac{1}{\tau} + \frac{\sigma^2}{2})t + \sigma W(t)} \left(Y_0 + \mu \int_0^t e^{(\frac{1}{\tau} + \frac{\sigma^2}{2})s - \sigma W(s)} ds \right). \quad (2)$$

Conditional and asymptotic mean and variance Since Y_0 has finite second moment, the mean and variance of the strong solution process Y , conditioned on the initial value Y_0 , exist. They are explicitly known [6, 18, 52] and given by

$$\mathbb{E}[Y(t)|Y_0] = Y_0 e^{-\frac{1}{\tau}t} + \mu\tau(1 - e^{-\frac{1}{\tau}t}), \quad (3)$$

$$\text{Var}(Y(t)|Y_0) = \begin{cases} e^{-\frac{1}{\tau}t} (2\mu[tY_0 - \tau Y_0 - t\mu\tau] + Y_0^2) \\ \quad - e^{-\frac{2}{\tau}t} (Y_0 - \mu\tau)^2 + (\mu\tau)^2, & \text{if } \sigma^2\tau = 1, \\ e^{-\frac{1}{\tau}t} (4\mu\tau[\mu\tau - Y_0]) - e^{-\frac{2}{\tau}t} (Y_0 - \mu\tau)^2 \\ \quad + 2\mu^2\tau t - 3(\mu\tau)^2 + 2\mu\tau Y_0 + Y_0^2, & \text{if } \sigma^2\tau = 2, \\ \frac{(\mu\tau)^2\sigma^2\tau}{2-\sigma^2\tau} + 2\tau\sigma^2\frac{(Y_0-\mu\tau)\mu\tau}{1-\sigma^2\tau} e^{-\frac{1}{\tau}t} - e^{-\frac{2}{\tau}t}(Y_0 - \mu\tau)^2 \\ \quad + e^{(\sigma^2-\frac{2}{\tau})t} \left[Y_0^2 - \frac{2Y_0\mu\tau}{1-\sigma^2\tau} + \frac{2(\mu\tau)^2}{(2-\sigma^2\tau)(1-\sigma^2\tau)} \right], & \text{otherwise.} \end{cases} \quad (4)$$

From (3), it follows that the asymptotic mean of Y exists. It is given by

$$\mathbb{E}[Y_\infty] := \lim_{t \rightarrow \infty} \mathbb{E}[Y(t)|Y_0] = \mu\tau. \quad (5)$$

From (4), it follows that, under the condition $\sigma^2\tau < 2$, the asymptotic variance of Y exists. It is given by

$$\text{Var}(Y_\infty) := \lim_{t \rightarrow \infty} \text{Var}(Y(t)|Y_0) = \frac{(\mu\tau)^2}{\frac{2}{\sigma^2\tau} - 1}. \quad (6)$$

Boundary properties Depending on the parameter μ , the IGBM possesses different properties at the boundary 0 according to Feller's boundary classification [27]. In particular, if $\mu = 0$ and $Y_0 > 0$, the boundary 0 is unattainable and attracting, i.e., the process cannot reach 0 in finite time, but is attracted to it as time tends to infinity. In the case that $\mu = Y_0 = 0$, the process is absorbed at the boundary immediately. If $\mu > 0$, then 0 is an entrance boundary, i.e., the process cannot reach the boundary in finite time if $Y_0 > 0$ or it immediately leaves 0 and stays above it if $Y_0 = 0$. If $\mu < 0$, the boundary is of exit type, i.e., the process can reach the boundary in finite time and, as soon as it attains the boundary, it leaves $[0, +\infty)$ and cannot return into it. In many applications the process is stopped when it reaches an exit boundary, such that its state space is $[0, +\infty)$.

Feller's boundary classification is based on the idea of transforming the one-dimensional diffusion into a Wiener process, first by a change of space (through the scale density) and second by a change of time (through the speed density). The scale and speed densities are given by

$$\begin{aligned} s(y) &:= e^{-\int_{y_0}^y \frac{2F(z)}{G^2(z)} dz} = s_0 e^{2\mu/\sigma^2 y} y^{2/\sigma^2\tau}, \quad s_0 = e^{-2\mu/\sigma^2 y_0} y_0^{-2/\sigma^2\tau}, \\ m(y) &:= \frac{1}{G^2(y)s(y)} = m_0 y^{-(2+2/\sigma^2\tau)} e^{-2\mu/\sigma^2 y}, \quad m_0 = s_0^{-1} \sigma^{-2}, \end{aligned}$$

respectively, where $y_0 > 0$ and F and G denote the drift and diffusion coefficients defined in (1). Further, the scale function is defined by

$$S[x_0, x] := \int_{x_0}^x s(y) dy,$$

where $x_0 > 0$. For the IGBM, the nature of the boundary 0 is uniquely determined by the three quantities

$$S(0, x] := \lim_{x_0 \rightarrow 0} S[x_0, x], \quad \Sigma_0 := \int_0^\epsilon S(0, x] m(x) dx, \quad N_0 := \int_0^\epsilon S[x, \epsilon] m(x) dx,$$

where $\epsilon > 0$ arbitrary. If $\mu = 0$, then $S(0, x] < \infty$, $\Sigma_0 = \infty$ and $N_0 = \infty$. If $\mu > 0$, then $S(0, x] = \infty$, $\Sigma_0 = \infty$ and $N_0 < \infty$. If $\mu < 0$, then $S(0, x] < \infty$, $\Sigma_0 < \infty$ and $N_0 = \infty$. This

implies the different types of boundary behaviour explained above, see Table 6.2 in [27]. According to this classification, we define the following properties, which are satisfied by the IGBM:

- *Unattainable property*: If $\mu \geq 0$, then $\mathbb{P}(Y(t) > 0 \text{ for all } t \geq 0 | Y_0 > 0) = 1$.
- *Absorbing property*: If $\mu = 0$, then $\mathbb{P}(Y(t) = 0 \text{ for all } t \geq 0 | Y_0 = 0) = 1$.
- *Entrance property*: If $\mu > 0$, then $\mathbb{P}(Y(t) > 0 \text{ for all } t > 0 | Y_0 = 0) = 1$.
- *Exit property*: If $\mu < 0$, then $\mathbb{P}(Y(t) < 0 \text{ for all } t > 0 | Y_0 \leq 0) = 1$.

3 Numerical methods for the IGBM

Consider a discretised time interval $[0, t_{\max}]$, $t_{\max} > 0$, with equidistant time steps $\Delta = t_i - t_{i-1}$, $i = 1, \dots, N$, $N \in \mathbb{N}$, $t_0 = 0$ and $t_N = t_{\max}$. We denote by $\tilde{Y}(t_i)$ a numerical realisation of the process Y at discrete time points $t_i = i\Delta$, where $\tilde{Y}(t_0) := Y_0$. In the following, we first recall the Euler-Maruyama and the Milstein schemes, and then we derive four additional schemes that are based on the numerical splitting approach.

3.1 Euler-Maruyama and Milstein schemes

Well-known methods to generate the data points $\tilde{Y}(t_i)$ are the Euler-Maruyama and the Milstein schemes [29, 38]. The Euler-Maruyama method yields trajectories of the IGBM through

$$\tilde{Y}^E(t_i) = \tilde{Y}^E(t_{i-1}) + \Delta \left(-\frac{1}{\tau} \tilde{Y}^E(t_{i-1}) + \mu \right) + \sigma \tilde{Y}^E(t_{i-1}) \xi_{i-1}, \quad (7)$$

where ξ_{i-1} are independent and identically distributed (iid) normal random variables with null mean and variance Δ , i.e., $\xi_{i-1} \sim \mathcal{N}(0, \Delta)$. The Milstein method yields trajectories of the IGBM via

$$\tilde{Y}^M(t_i) = \tilde{Y}^M(t_{i-1}) + \Delta \left(-\frac{1}{\tau} \tilde{Y}^M(t_{i-1}) + \mu \right) + \sigma \tilde{Y}^M(t_{i-1}) \left(\xi_{i-1} + \frac{\sigma}{2} (\xi_{i-1}^2 - \Delta) \right). \quad (8)$$

3.2 The splitting approach

We provide a brief account of the key ideas of the splitting method [7, 31, 37, 40] for an Itô SDE of the form

$$dY(t) = F(t, Y(t))dt + G(t, Y(t))dW(t), \quad t \geq 0, \quad Y(0) = Y_0, \quad (9)$$

where the drift coefficient and the diffusion component can be expressed as

$$F(t, Y(t)) = \sum_{l=1}^d F^{[l]}(t, Y(t)), \quad G(t, Y(t)) = \sum_{l=1}^d G^{[l]}(t, Y(t)), \quad d \in \mathbb{N}.$$

Usually, there are several ways to decompose the components F and G . The goal is to obtain subequations

$$dY(t) = F^{[l]}(t, Y(t))dt + G^{[l]}(t, Y(t))dW(t), \quad l \in \{1, \dots, d\}, \quad (10)$$

which can be solved explicitly. Once the explicit solutions are derived, they need to be composed. Two common procedures for doing this are the Lie-Trotter and the Strang approach [37, 49].

Let $\varphi_t^{[l]}(Y_0)$ denote the exact flows (solutions) of the subequations in (10) at time t and starting from Y_0 . Then, the Lie-Trotter composition of flows

$$\tilde{Y}(t_i) = \left(\varphi_{\Delta}^{[1]} \circ \dots \circ \varphi_{\Delta}^{[d]} \right) (\tilde{Y}(t_{i-1}))$$

and the Strang approach

$$\tilde{Y}(t_i) = \left(\varphi_{\Delta/2}^{[1]} \circ \dots \circ \varphi_{\Delta/2}^{[d-1]} \circ \varphi_{\Delta}^{[d]} \circ \varphi_{\Delta/2}^{[d-1]} \circ \dots \circ \varphi_{\Delta/2}^{[1]} \right) (\tilde{Y}(t_{i-1}))$$

yield numerical schemes for (9). The order of the evaluations of the exact flows can be changed, yielding different schemes within each approach.

3.2.1 Splitting schemes for the IGBM

With the purpose of excluding the inhomogeneous part, relying thus on the underlying GBM, we split (1) into two simple subequations, namely

$$\begin{aligned} dY(t) &= \underbrace{-\frac{1}{\tau}Y(t) dt}_{F^{[1]}(Y(t))} + \underbrace{\sigma Y(t) dW(t)}_{G^{[1]}(Y(t))}, \\ dY(t) &= \underbrace{\mu dt}_{F^{[2]}}, \quad G^{[2]} \equiv 0. \end{aligned}$$

The first equation, corresponding to the GBM, allows for an exact simulation of sample paths through

$$Y(t_i) = \varphi_{\Delta}^{[1]}(Y(t_{i-1})) = Y(t_{i-1})e^{-(\frac{1}{\tau} + \frac{\sigma^2}{2})\Delta + \sigma\xi_{i-1}}, \quad i = 1, \dots, N, \quad (11)$$

with iid random variables $\xi_{i-1} \sim \mathcal{N}(0, \Delta)$. The second equation is a simple ODE with its explicit solution given by

$$Y(t_i) = \varphi_{\Delta}^{[2]}(Y(t_{i-1})) = Y(t_{i-1}) + \mu\Delta, \quad i = 1, \dots, N.$$

The Lie-Trotter composition yields

$$\tilde{Y}^{L1}(t_i) := \left(\varphi_{\Delta}^{[1]} \circ \varphi_{\Delta}^{[2]} \right) (\tilde{Y}^{L1}(t_{i-1})) = e^{-(\frac{1}{\tau} + \frac{\sigma^2}{2})\Delta + \sigma\xi_{i-1}} \left(\tilde{Y}^{L1}(t_{i-1}) + \mu\Delta \right), \quad (12)$$

$$\tilde{Y}^{L2}(t_i) := \left(\varphi_{\Delta}^{[2]} \circ \varphi_{\Delta}^{[1]} \right) (\tilde{Y}^{L2}(t_{i-1})) = \tilde{Y}^{L2}(t_{i-1})e^{-(\frac{1}{\tau} + \frac{\sigma^2}{2})\Delta + \sigma\xi_{i-1}} + \mu\Delta, \quad (13)$$

and the Strang approach results in

$$\begin{aligned} \tilde{Y}^{S1}(t_i) &:= \left(\varphi_{\Delta/2}^{[2]} \circ \varphi_{\Delta}^{[1]} \circ \varphi_{\Delta/2}^{[2]} \right) (\tilde{Y}^{S1}(t_{i-1})) \\ &= \left(\tilde{Y}^{S1}(t_{i-1}) + \mu\frac{\Delta}{2} \right) e^{-(\frac{1}{\tau} + \frac{\sigma^2}{2})\Delta + \sigma\xi_{i-1}} + \mu\frac{\Delta}{2}, \end{aligned} \quad (14)$$

$$\begin{aligned} \tilde{Y}^{S2}(t_i) &:= \left(\varphi_{\Delta/2}^{[1]} \circ \varphi_{\Delta}^{[2]} \circ \varphi_{\Delta/2}^{[1]} \right) (\tilde{Y}^{S2}(t_{i-1})) \\ &= \tilde{Y}^{S2}(t_{i-1})e^{-(\frac{1}{\tau} + \frac{\sigma^2}{2})\Delta + \sigma(\varphi_{i-1} + \psi_{i-1})} + \mu\Delta e^{-(\frac{1}{\tau} + \frac{\sigma^2}{2})\frac{\Delta}{2} + \sigma\psi_{i-1}}, \end{aligned} \quad (15)$$

with iid random variables $\varphi_{i-1}, \psi_{i-1} \sim \mathcal{N}(0, \Delta/2)$. The equations (12)-(15) define four different numerical solutions of (1). If $\mu = 0$, the numerical solutions (12)-(15) coincide with the exact simulation scheme (11) for the GBM.

Remark 1. The numerical solutions (12)-(15) coincide with the discretised version of (2), where the integral is approximated using the left point rectangle rule, the right point rectangle rule, the trapezoidal rule and the midpoint rule, respectively.

4 Properties of the numerical schemes for the IGBM

We now examine the ability of the derived numerical methods to accurately preserve the properties of the process. In particular, we first provide closed-form expressions for their conditional and asymptotic means and variances and analyse the resulting biases. Then, we show how only the splitting schemes preserve the boundary properties of the IGBM.

4.1 Investigation of the conditional moments

The numerical solutions defined by (7), (8), (12)-(15) enable to express $\tilde{Y}(t_i)$ in terms of the initial value Y_0 . Indeed, by performing back iteration, we obtain

$$\tilde{Y}^E(t_i) = Y_0 \prod_{j=1}^i \left(1 - \frac{\Delta}{\tau} + \sigma \xi_{i-j}\right) + \mu \Delta \sum_{k=1}^{i-1} \prod_{j=1}^k \left(1 - \frac{\Delta}{\tau} + \sigma \xi_{i-j}\right) + \mu \Delta, \quad (16)$$

$$\begin{aligned} \tilde{Y}^M(t_i) &= Y_0 \prod_{j=1}^i \left(1 - \frac{\Delta}{\tau} + \sigma \xi_{i-j} + (\xi_{i-j}^2 - \Delta) \frac{\sigma^2}{2}\right) \\ &\quad + \mu \Delta \sum_{k=1}^{i-1} \prod_{j=1}^k \left(1 - \frac{\Delta}{\tau} + \sigma \xi_{i-j} + (\xi_{i-j}^2 - \Delta) \frac{\sigma^2}{2}\right) + \mu \Delta, \end{aligned} \quad (17)$$

$$\tilde{Y}^{L1}(t_i) = Y_0 e^{-(\frac{1}{\tau} + \frac{\sigma^2}{2})t_i + \sigma \sum_{k=0}^{i-1} \xi_k} + \mu \Delta \sum_{k=1}^i e^{-(\frac{1}{\tau} + \frac{\sigma^2}{2})t_k + \sigma \sum_{j=1}^k \xi_{i-j}}, \quad (18)$$

$$\tilde{Y}^{L2}(t_i) = Y_0 e^{-(\frac{1}{\tau} + \frac{\sigma^2}{2})t_i + \sigma \sum_{k=0}^{i-1} \xi_k} + \mu \Delta \sum_{k=1}^{i-1} e^{-(\frac{1}{\tau} + \frac{\sigma^2}{2})t_k + \sigma \sum_{j=1}^k \xi_{i-j}} + \mu \Delta, \quad (19)$$

$$\tilde{Y}^{S1}(t_i) = \left(Y_0 + \frac{\mu \Delta}{2}\right) e^{-(\frac{1}{\tau} + \frac{\sigma^2}{2})t_i + \sigma \sum_{k=0}^{i-1} \xi_k} + \mu \Delta \sum_{k=1}^{i-1} e^{-(\frac{1}{\tau} + \frac{\sigma^2}{2})t_k + \sigma \sum_{j=1}^k \xi_{i-j}} + \frac{\mu \Delta}{2}, \quad (20)$$

$$\tilde{Y}^{S2}(t_i) = Y_0 e^{-(\frac{1}{\tau} + \frac{\sigma^2}{2})t_i + \sigma \sum_{k=0}^{i-1} \xi_k} + \mu \Delta \sum_{k=1}^i e^{-(\frac{1}{\tau} + \frac{\sigma^2}{2})(k - \frac{1}{2})\Delta + \sigma \psi_{i-k} + \sigma \sum_{j=1}^{k-1} \xi_{i-j}}, \quad (21)$$

where $\xi_i := \varphi_i + \psi_i$ in (21). These relations allow for an investigation of the conditional means $\mathbb{E}[\tilde{Y}(t_i)|Y_0]$ and variances $\text{Var}(\tilde{Y}(t_i)|Y_0)$ of the numerical solutions.

4.1.1 Closed-form expressions for the conditional means and variances

In Proposition 1, we provide closed-form expressions of the conditional mean and variance of a general random variable Z_i that plays the role of a numerical solution $\tilde{Y}(t_i)$ as in (16)-(21) for a fixed time t_i . These expressions will allow for a straightforward derivation of the corresponding results for the numerical solutions of interest.

Proposition 1. Consider the real-valued random variable Z_i defined by

$$Z_i := Z_0 W_i + c_1 \sum_{k=0}^I W_k H_{k+1} + c_2, \quad (22)$$

where $i \in \mathbb{N}$, $I \in \{i-1, i\}$, $c_1, c_2 > 0$, $Z_0 \in \mathbb{R}$, $W_0 \in \{0, 1\}$, $W_k := \prod_{j=1}^k X_j$ with $X_j := M_j H_j$, $j = 1, \dots, k$, being iid random variables with mean $\mu_x \in \mathbb{R}$ and second moment $r > 0$. The random variables M_j and H_j are iid with means $\mu_m, \mu_h \in \mathbb{R}$ and second moments $r_m, r_h > 0$. The mean of Z_i conditioned on Z_0 is given by

$$\mathbb{E}[Z_i|Z_0] = Z_0 \mu_x^i + c_1 \mu_h \sum_{k=1}^I \mu_x^k + c_1 W_0 \mu_h + c_2 \quad (23)$$

and the variance of Z_i conditioned on Z_0 is given by

$$\begin{aligned} \text{Var}(Z_i|Z_0) &= Z_0^2 (r^i - \mu_x^{2i}) + 2c_1 Z_0 \sum_{k=0}^I (r^k r_h - \mu_x^{2k} \mu_h^2) \mu_m \mu_x^{i-k-1} \\ &\quad + c_1^2 \left[\sum_{k=0}^I (r^k r_h - \mu_x^{2k} \mu_h^2) + 2 \sum_{l=1}^I \sum_{k=0}^{l-1} (r^k r_h - \mu_x^{2k} \mu_h^2) \mu_m \mu_h \mu_x^{l-k-1} \right]. \quad (24) \end{aligned}$$

The proof of Proposition 1 is given in Appendix A.

Based on Proposition 1, we derive the conditional moments of the Euler-Maruyama, Milstein and splitting schemes.

Corollary 1. Let $\tilde{Y}(t_i)$ be the numerical solutions defined through (7), (8) and (12)-(15), respectively, at time $t_i = i\Delta$. Their means and variances conditioned on the initial value Y_0 are given by (23) and (24), respectively, with quantities μ_x , μ_h , μ_m , r , r_h , r_m , c_1 , c_2 , I , Z_0 and W_0 defined as reported in Table 1.

The proof of Corollary 1 is given in Appendix B.

While the conditional means of the Euler-Maruyama and Milstein schemes are equal, their conditional variances are different. This results from the fact that the Milstein scheme takes into account an additional term that is related only to the diffusion coefficient of the SDE. Noting that $\mu\Delta = \mu\tau\Delta/\tau$, it can be observed that all conditional means depend on Δ/τ and all conditional variances depend on Δ/τ and $\Delta\sigma^2$. If $\mu = 0$, the conditional means and variances of the splitting solutions (12)-(15) coincide with the true quantities (3) and (4), respectively, at time t_i .

Table 1: Quantities of interest for the numerical schemes entering in (23)-(24).

Z_i	μ_x	μ_h	μ_m	r	r_h	r_m	c_1	c_2	I	Z_0	W_0
$\tilde{Y}^E(t_i)$	$1 - \frac{\Delta}{\tau}$	1	μ_x	$\sigma^2 \Delta + (1 - \frac{\Delta}{\tau})^2$	1	r	$\mu\Delta$	$\mu\Delta$	$i-1$	Y_0	0
$\tilde{Y}^M(t_i)$	$1 - \frac{\Delta}{\tau}$	1	μ_x	$\sigma^2 \Delta + (1 - \frac{\Delta}{\tau})^2 + \frac{(\sigma^2 \Delta)^2}{2}$	1	r	$\mu\Delta$	$\mu\Delta$	$i-1$	Y_0	0
$\tilde{Y}^{L1}(t_i)$	$e^{-\Delta/\tau}$	1	μ_x	$e^{\sigma^2 \Delta - 2\Delta/\tau}$	1	r	$\mu\Delta$	0	i	Y_0	0
$\tilde{Y}^{L2}(t_i)$	$e^{-\Delta/\tau}$	1	μ_x	$e^{\sigma^2 \Delta - 2\Delta/\tau}$	1	r	$\mu\Delta$	$\mu\Delta$	$i-1$	Y_0	0
$\tilde{Y}^{S1}(t_i)$	$e^{-\Delta/\tau}$	1	μ_x	$e^{\sigma^2 \Delta - 2\Delta/\tau}$	1	r	$\mu\Delta$	$\frac{\mu\Delta}{2}$	$i-1$	$Y_0 + \frac{\mu\Delta}{2}$	0
$\tilde{Y}^{S2}(t_i)$	$e^{-\Delta/\tau}$	$\mu_x^{1/2}$	$\mu_x^{1/2}$	$e^{\sigma^2 \Delta - 2\Delta/\tau}$	$r^{1/2}$	$r^{1/2}$	$\mu\Delta$	0	$i-1$	Y_0	1

Remark 2. Having a closed-form expression for the conditional moments of the numerical solutions allows for a direct control of the introduced errors through the choice of the time discretisation step Δ .

4.1.2 Conditional mean and variance biases

Corollary 1 implies that all numerical methods yield conditional means and variances different from the true values. In the following, we study the introduced relative mean and variance biases defined by

$$\text{rBias}_{\Delta,t_i,Y_0}(\mathbb{E}[\tilde{Y}]) := \frac{\mathbb{E}[\tilde{Y}(t_i)|Y_0] - \mathbb{E}[Y(t_i)|Y_0]}{\mathbb{E}[Y(t_i)|Y_0]}, \quad (25)$$

$$\text{rBias}_{\Delta,t_i,Y_0}(\text{Var}(\tilde{Y})) := \frac{\text{Var}(\tilde{Y}(t_i)|Y_0) - \text{Var}(Y(t_i)|Y_0)}{\text{Var}(Y(t_i)|Y_0)}, \quad (26)$$

for each considered numerical method. These biases depend on the time step Δ , the time t_i , the initial condition Y_0 and the parameters of the model. While the biases in the conditional variance depend on all model parameters, the biases in the conditional means do not depend on σ .

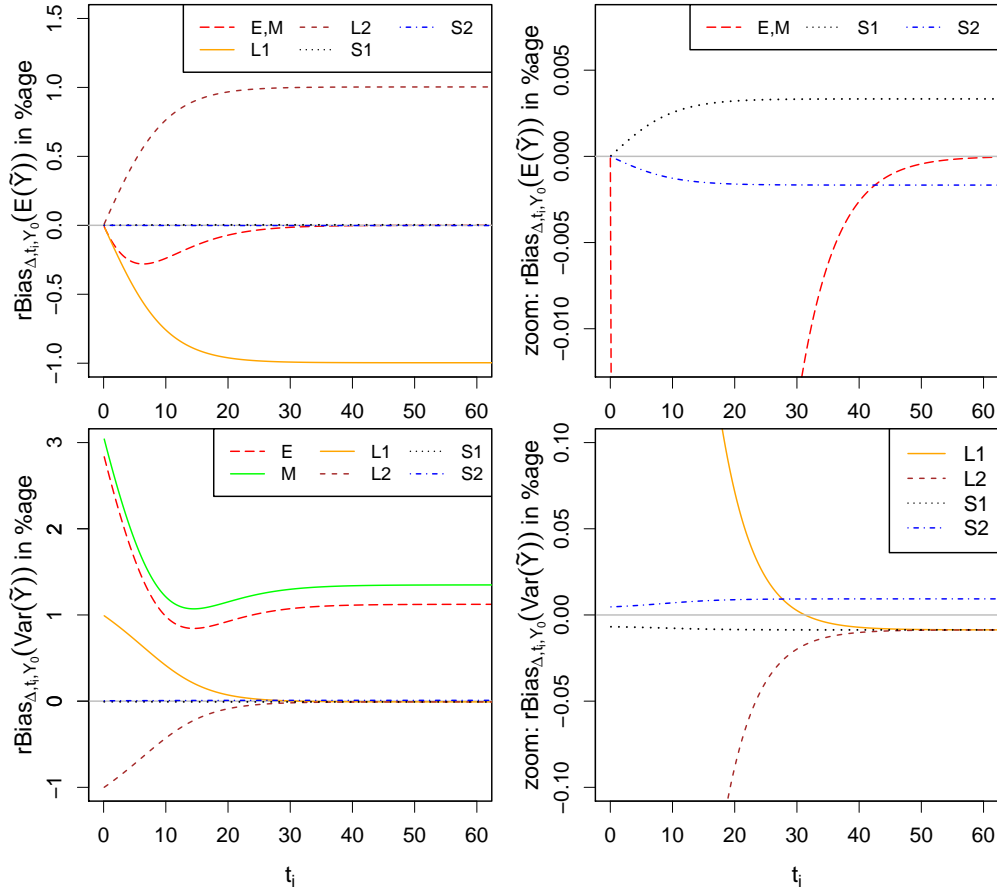


Figure 1: The relative conditional mean bias (25) (top left panel for E,M,L1,L2,S1,S2 and a zoom in the top right panel for E,M,S1,S2) and conditional variance bias (26) (bottom left panel for E,M,L1,L2,S1,S2 and a zoom in the bottom right panel for L1,L2,S1,S2) in percentage as a function of the time t_i , for $Y_0 = 10$, $\Delta = 0.1$, $\mu = 1$, $\tau = 5$ and $\sigma = 0.2$.

In the top left panel of Figure 1, we report the relative mean bias (25) in percentage as a function of t_i , for $Y_0 = 10$, $\Delta = 0.1$, $\mu = 1$ and $\tau = 5$. The relative mean biases (in absolute value) introduced by the Strang splitting schemes are significantly smaller than those of the Lie-Trotter splitting schemes and close to 0 for all t_i under consideration, with the second Strang scheme performing slightly better than the first one (see top right panel). Furthermore, in the non-stationary initial part, the Strang splitting schemes clearly outperform the Euler-Maruyama and Milstein schemes. This changes with increasing time, as it can be observed in the top right panel, where we provide a zoom. In particular, for $t_i \approx 43$, the Euler-Maruyama and Milstein schemes start to outperform the Strang splitting schemes, with a relative bias approaching 0, suggesting an asymptotically unbiased mean (see Section 4.2).

In the bottom left panel of Figure 1, we report the conditional variance biases (26) in percentage as a function of t_i for the same values of Y_0 , Δ , μ and τ as before and $\sigma = 0.2$. All four splitting schemes yield better approximations of the conditional variance than the Euler-Maruyama and Milstein schemes for all t_i under consideration. While the Strang splitting schemes yield again biases close to 0 from the beginning, the relative variance biases (in absolute value) of the Lie-Trotter splitting schemes decrease in time and seem to coincide asymptotically with that of the first Strang scheme (see Section 4.2), as it can be observed in the bottom right panel of Figure 1, where we provide a zoom. Similar results are obtained for other parameters, time steps and initial values.

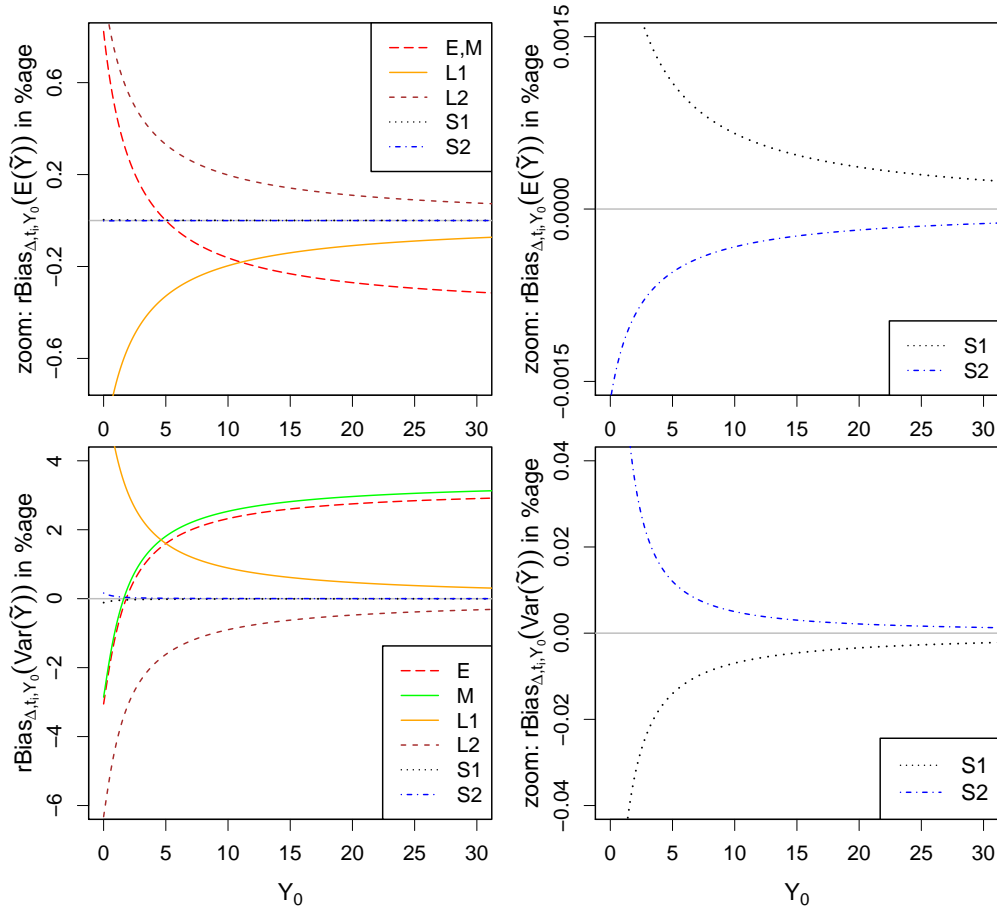


Figure 2: The relative conditional mean bias (25) (top left panel for E,M,L1,L2,S1,S2 and a zoom in the top right panel for S1,S2) and conditional variance bias (26) (bottom left panel for E,M,L1,L2,S1,S2 and a zoom in the bottom right panel for S1,S2) in percentage as a function of the initial value Y_0 , for $t_i = 2$, $\Delta = 0.1$, $\mu = 1$, $\tau = 5$ and $\sigma = 0.2$.

In Figure 2, we report the relative biases of the conditional mean (25) (top panels) and variance (26) (bottom panels) in percentage as a function of the initial value Y_0 , for $t_i = 2$ and the same parameters as before. The Strang splitting schemes (zooms are provided in the right panels) outperform the other methods, yielding relative biases close to 0 for any considered choice of the initial condition, not being strongly influenced by it. The performance of the splitting schemes improves as Y_0 increases, while the Euler-Maruyama and Milstein schemes perform worse for large values of Y_0 . Moreover, the conditional mean biases (not the relative ones) of the splitting schemes do not depend on Y_0 , while those of the other schemes do. Furthermore, the conditional variance biases introduced by the splitting schemes depend linearly on Y_0 , while those of the Euler-Maruyama and Milstein schemes depend quadratically on Y_0 . If Y_0 is close to the asymptotic mean $\mu\tau$, here 5, the relative mean bias of the Euler-Maruyama and Milstein schemes is almost 0 (top left panel), in agreement with the fact that they have an asymptotically unbiased mean (see Section 4.2).

4.2 Investigation of the asymptotic moments

We now investigate the asymptotic mean and variance of the numerical solutions, i.e.,

$$\mathbb{E}[\tilde{Y}_\infty] := \lim_{i \rightarrow \infty} \mathbb{E}[\tilde{Y}(t_i)|Y_0], \quad \text{Var}(\tilde{Y}_\infty) := \lim_{i \rightarrow \infty} \text{Var}(\tilde{Y}(t_i)|Y_0), \quad t_i = i\Delta,$$

comparing them with the true quantities (5) and (6), respectively.

4.2.1 Closed-form expressions for the asymptotic means and variances

In Proposition 2, we provide closed-form expressions of the asymptotic mean and variance of the random variable Z_i introduced in Proposition 1. As before, these relations allow for a straightforward derivation of the corresponding results for the numerical schemes of interest, including necessary conditions that guarantee the existence of the asymptotic quantities.

Proposition 2. *Let the random variable Z_i be defined as in Proposition 1. If $|\mu_x| < 1$, the asymptotic mean of Z_i is given by*

$$\mathbb{E}[Z_\infty] := \lim_{i \rightarrow \infty} \mathbb{E}[Z_i|Z_0] = c_1 \mu_h \frac{\mu_x}{1 - \mu_x} + c_1 W_0 \mu_h + c_2. \quad (27)$$

If, in addition, $r \in (0, 1)$, the asymptotic variance of Z_i is given by

$$\text{Var}(Z_\infty) := \lim_{i \rightarrow \infty} \text{Var}(Z_i|Z_0) = c_1^2 \frac{(1 + \mu_h \mu_m)[r_h(\mu_x^2 - 1) - \mu_h^2(r - 1)]}{(\mu_x - 1)^2(1 + \mu_x)(r - 1)}. \quad (28)$$

The proof of Proposition 2 is given in Appendix C.

Based on Proposition 2, we derive the asymptotic moments of the Euler-Maruyama, Milstein and splitting schemes.

Corollary 2. *Let $\tilde{Y}(t_i)$ be the numerical solutions defined through (7), (8) and (12)-(15), respectively. The asymptotic means and variances of the Euler-Maruyama and Milstein schemes are given by*

$$\text{If } \left| 1 - \frac{\Delta}{\tau} \right| < 1, \quad \mathbb{E}[\tilde{Y}_\infty^E] = \mathbb{E}[\tilde{Y}_\infty^M] = \mu\tau, \quad (29)$$

$$\text{If } \left| 1 - \frac{\Delta}{\tau} \right| < 1 \text{ and } \Delta < 2\tau - \sigma^2\tau^2, \quad \text{Var}(\tilde{Y}_\infty^E) = \frac{(\mu\tau)^2}{\frac{2}{\sigma^2\tau} - 1 - \frac{\Delta}{\sigma^2\tau^2}}, \quad (30)$$

$$\text{If } \left| 1 - \frac{\Delta}{\tau} \right| < 1 \text{ and } \Delta < \frac{2\tau - \sigma^2\tau^2}{\frac{\sigma^4\tau^2}{2} + 1}, \quad \text{Var}(\tilde{Y}_\infty^M) = \frac{(\mu\tau)^2(1 + \frac{\sigma^2\Delta}{2})}{\frac{2}{\sigma^2\tau} - 1 - \frac{\Delta}{\sigma^2\tau^2} - \frac{\sigma^2\Delta}{2}}. \quad (31)$$

The asymptotic means and variances of the splitting schemes are given by

$$\mathbb{E}[\tilde{Y}_\infty^{L1}] = \mu\tau \left[\frac{\Delta/\tau}{-1 + e^{\Delta/\tau}} \right], \quad (32)$$

$$\mathbb{E}[\tilde{Y}_\infty^{L2}] = \mathbb{E}[\tilde{Y}_\infty^{L1}] + \mu\Delta = \mathbb{E}[\tilde{Y}_\infty^{L1}]e^{\Delta/\tau}, \quad (33)$$

$$\mathbb{E}[\tilde{Y}_\infty^{S1}] = \mathbb{E}[\tilde{Y}_\infty^{L1}] + \frac{1}{2}\mu\Delta = \frac{1}{2}\mathbb{E}[\tilde{Y}_\infty^{L1}](1 + e^{\Delta/\tau}), \quad (34)$$

$$\mathbb{E}[\tilde{Y}_\infty^{S2}] = \mathbb{E}[\tilde{Y}_\infty^{L1}]e^{\Delta/2\tau}, \quad (35)$$

$$\text{If } \sigma^2\tau < 2, \text{ } \text{Var}(\tilde{Y}_\infty^{L1}) = \text{Var}(\tilde{Y}_\infty^{L2}) = \text{Var}(\tilde{Y}_\infty^{S1}) = \mathbb{E}[\tilde{Y}_\infty^{L1}]^2 \frac{e^{2\Delta/\tau}(1 - e^{\Delta\sigma^2})}{e^{\Delta\sigma^2} - e^{2\Delta/\tau}}, \quad (36)$$

$$\text{If } \sigma^2\tau < 2, \text{ } \text{Var}(\tilde{Y}_\infty^{S2}) = \mathbb{E}[\tilde{Y}_\infty^{L1}]^2 \frac{e^{\Delta/\tau}(1 - e^{\Delta\sigma^2/2})(e^{2\Delta/\tau} + e^{\Delta\sigma^2/2})}{e^{\Delta\sigma^2} - e^{2\Delta/\tau}}. \quad (37)$$

Proof. The results and their required conditions follow directly from Proposition 2, using the corresponding values reported in Table 1 and simplifying the resulting expressions. \square

Remarkably, the splitting schemes do not require extra conditions for the existence of the asymptotic mean, as it is the case for the IGBM. Moreover, the condition guaranteeing the existence of the asymptotic variance of the splitting schemes and of the true process is the same, i.e., $\sigma^2\tau < 2$. In contrast, the Euler-Maruyama and the Milstein schemes rely on extra conditions that do not depend on the features of the model. If $|1 - \Delta/\tau| < 1$, the Euler-Maruyama and the Milstein schemes have unbiased asymptotic means. Regarding the asymptotic variance, the condition for the Milstein scheme in (31) is more restrictive than that for the Euler-Maruyama method in (30), agreeing with similar results in the literature [12]. The asymptotic variances of the Lie-Trotter schemes and the first Strang scheme coincide, as previously hypothesised looking at Figure 1.

If $\mu = 0$, the results for the Euler-Maruyama and Milstein methods in Corollary 2 are in agreement with those available for the GBM [23, 45]. In particular, the conditions required in (30) and (31) are the same as those guaranteeing their second moment stability. On the contrary, Corollary 2 implies that the numerical splitting solutions (12)-(15) are asymptotically first and second moment stable without needing extra conditions.

4.2.2 Asymptotic mean and variance biases

Corollary 2 implies that the derived schemes introduce asymptotic mean and variance biases. In the following, we analyse the resulting asymptotic relative biases

$$\text{rBias}_\Delta \left(\mathbb{E}[\tilde{Y}_\infty] \right) := \frac{\mathbb{E}[\tilde{Y}_\infty] - \mathbb{E}[Y_\infty]}{\mathbb{E}[Y_\infty]}, \quad (38)$$

$$\text{rBias}_\Delta \left(\text{Var}(\tilde{Y}_\infty) \right) := \frac{\text{Var}(\tilde{Y}_\infty) - \text{Var}(Y_\infty)}{\text{Var}(Y_\infty)}, \quad (39)$$

with respect to the true quantities (5) and (6), for each considered numerical method. These biases depend on the time step Δ and on the model parameters. All relative asymptotic biases do not depend on μ . In particular, the asymptotic mean biases depend only on the ratio Δ/τ and the asymptotic variance biases depend on both Δ/τ and $\Delta\sigma^2$. Remarkably, all biases vanish as $\Delta \rightarrow 0$, provided that the conditions of Corollary 2 are satisfied.

In Figure 3, we report the relative biases of the asymptotic mean (top panels) and variance (bottom panels) in percentage as a function of the time step Δ , for $\tau = 5$ and different values of σ fulfilling the conditions of Corollary 2. Independent of the choice of the model parameters and for any time step $\Delta > 0$, the Strang splitting schemes yield significantly smaller asymptotic mean biases (in absolute value) than the Lie-Trotter splitting schemes, in agreement with the results reported in the previous section. Moreover, the mean bias (in absolute value) of the second Strang scheme is slightly smaller than that of the first Strang scheme as highlighted in the top right panel,

where we provide a zoom. All splitting schemes yield significantly smaller asymptotic variance biases (in absolute value) than the Euler-Maruyama and Milstein methods, as illustrated in the bottom panels of Figure 3. Note that, the Milstein scheme introduces slightly larger variance biases than the Euler-Maruyama method as highlighted in the bottom right panel of Figure 3.

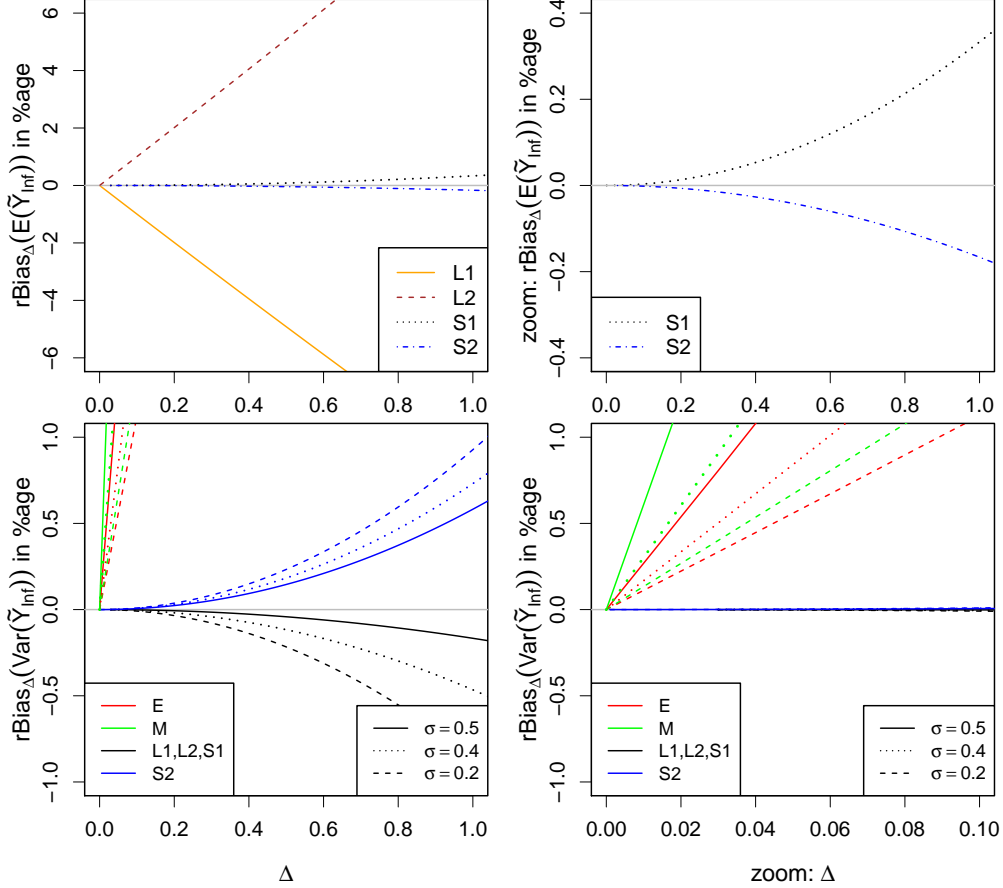


Figure 3: The relative asymptotic mean bias (38) (top left panel for L1,L2,S1,S2 and a zoom in the top right panel for S1,S2) and asymptotic variance bias (39) (bottom left panel and a zoom in the bottom right panel for E,M,L1,L2,S1,S2) in percentage as a function of the time step Δ , for $\tau = 5$ and different values of σ .

In Figure 4, we analyse how the performance of the numerical methods is affected by the model parameters. In the top left panel of Figure 4, we report the asymptotic relative mean biases of the splitting schemes in percentage as a function of the parameter τ (a zoom for the Strang schemes is provided in the top right panel). The asymptotic relative mean biases (in absolute value) decrease as τ increases, in agreement with the fact that they depend on the ratio Δ/τ . In the bottom left panel of Figure 4, we visualise the asymptotic relative variance biases of the considered numerical methods in percentage as a function of τ (a zoom for the splitting schemes is provided in the bottom right panel). While the relative variance biases (in absolute value) of the splitting schemes decrease as τ increases, those of the Euler-Maruyama and Milstein schemes initially decrease and then increase. Interestingly, while the relative asymptotic variance biases of the Euler-Maruyama and Milstein schemes increase in σ (bottom left panel), those of the splitting schemes (in absolute value) decrease as σ increases (bottom right panel). This can be also observed in the bottom panels of Figure 3. In general, if both τ and σ are large, such that the stationary condition $\sigma^2\tau < 2$ is only met tightly, the Euler-Maruyama and Milstein schemes seem to perform worse, while the splitting schemes improve as both τ and σ increase.

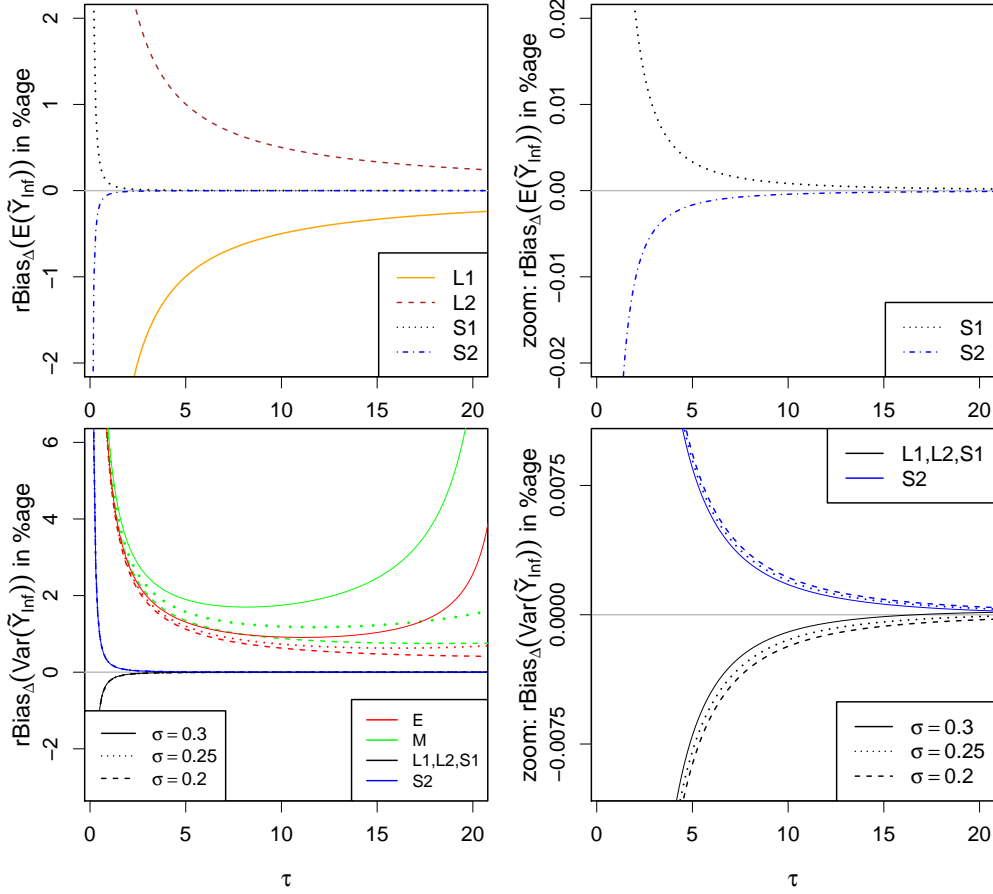


Figure 4: The relative asymptotic mean bias (38) (top left panel for L1,L2,S1,S2 and a zoom in the top right panel for S1,S2) and asymptotic variance bias (39) (bottom left panel for E,M,L1,L2,S1,S2 and a zoom in the bottom right panel for L1,L2,S1,S2) in percentage as a function of the parameter τ , for $\Delta = 0.1$ and different values of σ .

Even though the Strang splitting schemes perform slightly worse than the Euler-Maruyama and Milstein schemes in terms of the asymptotic mean, they clearly outperform them in terms of the asymptotic variance. For this reason, when, for example, analysing the asymptotic coefficient of variation, i.e., $\text{CV}(Y_\infty) := \sqrt{\text{Var}(Y_\infty)}/\mathbb{E}[Y_\infty]$, which is a measure of dispersion that allows to simultaneously study the error impinging on both quantities, the Strang splitting schemes are superior to all other schemes. Moreover, if the stationary condition $\sigma^2\tau < 2$ is only met tightly, the first Strang scheme outperforms the second one in terms of the CV.

4.3 Preservation of the boundary properties

As discussed in Section 2, the boundary 0 of the IGBM may be of entrance, unattainable and attracting or exit type, depending on the parameter μ . Corresponding properties motivated by this classification have been introduced at the end of Section 2. A numerical scheme $\tilde{Y}(t_i)$ is said to preserve these properties if the following discrete versions are fulfilled:

- *Discrete unattainable property*: If $\mu \geq 0$, then $\mathbb{P}(\tilde{Y}(t_i) > 0 | \tilde{Y}(t_{i-1}) > 0) = 1$.
- *Discrete absorbing property*: If $\mu = 0$, then $\mathbb{P}(\tilde{Y}(t_1) = 0 | Y_0 = 0) = 1$.
- *Discrete entrance property*: If $\mu > 0$, then $\mathbb{P}(\tilde{Y}(t_1) > 0 | Y_0 = 0) = 1$.
- *Discrete exit property*: If $\mu < 0$, then $\mathbb{P}(\tilde{Y}(t_i) < 0 | \tilde{Y}(t_{i-1}) \leq 0) = 1$.

It is well known that the Euler-Maruyama and Milstein schemes may fail in meeting such conditions. For example, the Euler-Maruyama scheme (7) does not fulfill the discrete unattainable property for any choice of Δ , since ξ_{i-1} assumes all values in \mathbb{R} with a positive probability [26]. Moreover, the Milstein scheme (8) may not fulfill this property either, if $\tilde{Y}(t_{i-1})(\sigma^2 + \frac{2}{\tau}) - 2\mu > 0$, unless the time discretisation step Δ satisfies

$$\Delta < \frac{2yG'(y) - G(y)}{(G(y)G'(y) - 2F(y))G'(y)} = \frac{y}{\sigma^2 y + \frac{2}{\tau} y - 2\mu}, \quad (40)$$

where $y := \tilde{Y}(t_{i-1})$ and $G'(y)$ denotes the derivative of G with respect to y [26]. Thus, to guarantee positivity, the time step Δ would need to be updated in every iteration step.

Note that, the discrete absorbing property is the only property which is satisfied by the Euler-Maruyama and Milstein schemes, for any time step Δ . In contrast, the derived splitting schemes preserve the different boundary properties for any choice of time step $\Delta > 0$, as shown below. Moreover, their boundary behaviour depends only on the parameter μ , as it is the case for the IGBM.

Proposition 3. *Let $\tilde{Y}(t_i)$ be the numerical splitting solutions defined through (12)-(15), respectively. They fulfill the discrete unattainable, absorbing, entrance and exit properties for any choice of the time step Δ .*

Proof. The properties can be easily verified from (12)-(15), using the corresponding assumptions on the parameter μ and the positivity of the exponential function. \square

5 Numerical experiments

We now illustrate the theoretical results of the numerical methods introduced in the previous section through a series of numerical experiments, focusing on the conditional and asymptotic moments and on the boundary properties. Moreover, we illustrate how the Strang splitting schemes yield better estimations of the stationary density of the process than all other schemes as Δ increases, and provide a further investigation of the boundary behaviour.

5.1 Conditional and asymptotic moments

Here, we illustrate that the conditional and asymptotic means and variances obtained via numerical simulations are in agreement with the previously derived theoretical expressions. To do so, we define the sample mean \hat{m}_{t_i} and variance \hat{v}_{t_i} as follows

$$\mathbb{E}[Y(t_i)|Y_0] \approx \mathbb{E}[\tilde{Y}(t_i)|Y_0] \approx \hat{m}_{t_i} := \frac{1}{n} \sum_{k=1}^n \tilde{Y}_k(t_i), \quad (41)$$

$$\text{Var}(Y(t_i)|Y_0) \approx \text{Var}(\tilde{Y}(t_i)|Y_0) \approx \hat{v}_{t_i} := \frac{1}{n-1} \sum_{k=1}^n \left(\tilde{Y}_k(t_i) - \hat{m}_{t_i} \right)^2, \quad (42)$$

where $\tilde{Y}_k(t_i)$ denotes the k -th simulated value of $Y(t_i)$ under each considered numerical method, respectively. We denote by $\text{RE}(\hat{m}_{t_i})$ and $\text{RE}(\hat{v}_{t_i})$ the relative biases (25) and (26), estimated replacing $\mathbb{E}[\tilde{Y}(t_i)|Y_0]$ and $\text{Var}(\tilde{Y}(t_i)|Y_0)$ with the sample mean (41) and variance (42), respectively. To investigate the asymptotic case, we fix $t_i = 100$ and denote by $\text{RE}(\hat{m}_{100})$ and $\text{RE}(\hat{v}_{100})$ the relative biases (38) and (39), estimated replacing $\mathbb{E}[\tilde{Y}_\infty]$ and $\text{Var}(\tilde{Y}_\infty)$ with \hat{m}_{100} and \hat{v}_{100} , respectively.

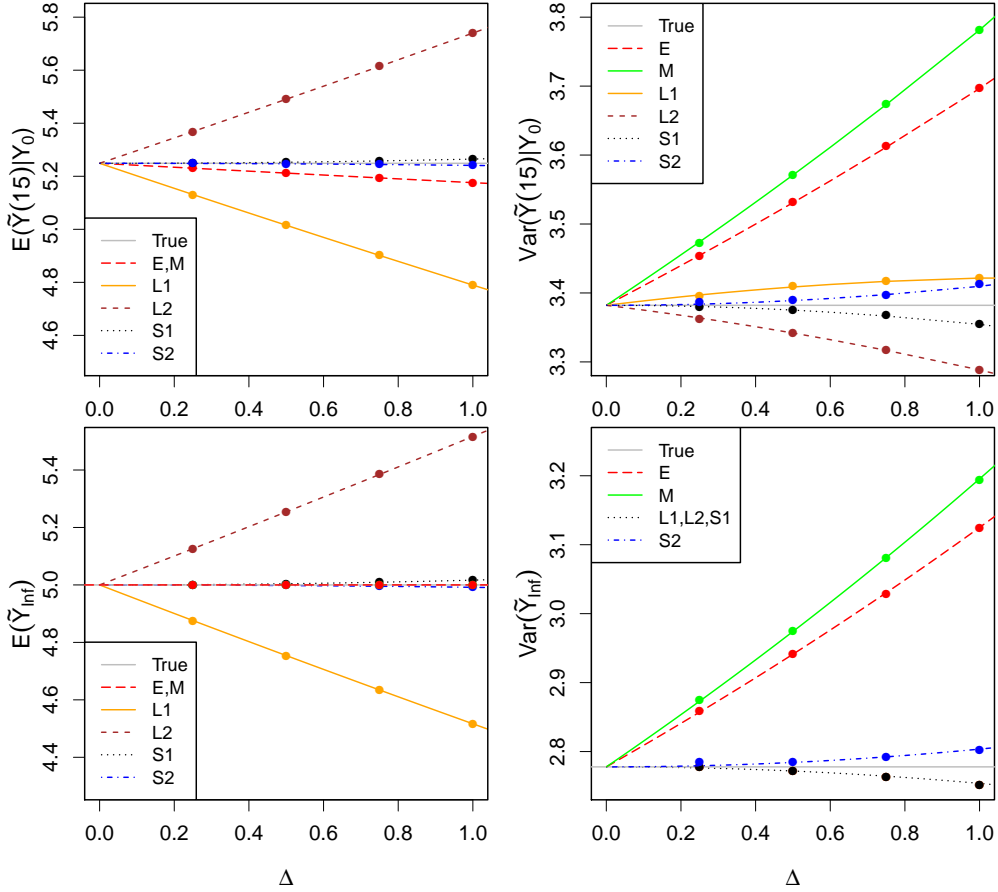


Figure 5: Dependence of the theoretical conditional mean $\mathbb{E}[\tilde{Y}(15)|Y_0]$ (top left panel), conditional variance $\text{Var}(\tilde{Y}(15)|Y_0)$ (top right panel), asymptotic mean $\mathbb{E}[\tilde{Y}_\infty]$ (bottom left panel) and asymptotic variance $\text{Var}(\tilde{Y}_\infty)$ (bottom right panel) on the time step Δ , for $\mu = 1$, $\tau = 5$, $\sigma = 0.2$ and initial value $Y_0 = 10$. The filled circles correspond to the sample mean \hat{m}_{15} (top left panel), sample variance \hat{v}_{15} (top right panel), sample mean \hat{m}_{100} (bottom left panel) and sample variance \hat{v}_{100} (bottom right panel), calculated for $\Delta = 0.25, 0.5, 0.75, 1$ and obtained from $n = 10^7$ simulations of $Y(15)$ and $Y(100)$, respectively, using the different numerical methods. The true conditional mean $\mathbb{E}[Y(15)|Y_0]$, conditional variance $\text{Var}(Y(15)|Y_0)$, asymptotic mean $\mathbb{E}[Y_\infty]$ and asymptotic variance $\text{Var}(Y_\infty)$ are represented by the grey horizontal lines.

In the top panels of Figure 5, we fix $t_i = 15$ and report the true conditional mean $\mathbb{E}[Y(15)|Y_0]$ (3) and variance $\text{Var}(Y(15)|Y_0)$ (4) (grey horizontal lines), the theoretical conditional means $\mathbb{E}[\tilde{Y}(15)|Y_0]$ (23) and variances $\text{Var}(\tilde{Y}(15)|Y_0)$ (24) of the numerical methods as a function of the time step Δ and their estimated values (filled circles) \hat{m}_{15} (41) and \hat{v}_{15} (42), derived for $\Delta = 0.25, 0.5, 0.75, 1$. We calculate the sample moments from $n = 10^7$ simulations of $Y(15)$, for $\mu = 1$, $\tau = 5$, $\sigma = 0.2$ and $Y_0 = 10$. In the bottom panels of Figure 5, we report the true asymptotic mean $\mathbb{E}[Y_\infty]$ (5) and variance $\text{Var}(Y_\infty)$ (6) (grey horizontal lines), the theoretical asymptotic means $\mathbb{E}[\tilde{Y}_\infty]$ (29), (32)-(35) and variances $\text{Var}(\tilde{Y}_\infty)$ (30), (31), (36), (37) as a function of the time step Δ and their estimated values (filled circles) \hat{m}_{100} (41) and \hat{v}_{100} (42). The corresponding relative biases $\text{RE}(\hat{m}_{15})$, $\text{RE}(\hat{v}_{15})$, $\text{RE}(\hat{m}_{100})$ and $\text{RE}(\hat{v}_{100})$ in percentage, for $\Delta = 0.5$ and $\Delta = 1$ are reported in Table 2. The quantities obtained through numerical simulations are in agreement with the theoretical ones.

Table 2: Comparison of the theoretical quantities with those obtained via $n = 10^7$ simulations. We report the relative conditional mean and variance biases (25) and (26), the asymptotic mean and variance biases (38) and (39) (in parentheses) and 1000 times the KL divergences (44) for $\Delta = 0.5$ and $\Delta = 1$. The parameters are $\mu = 1$, $\tau = 5$, $\sigma = 0.2$ and $Y_0 = 10$.

$\Delta = 0.5$	$\text{RE}(\hat{m}_{15})$ in %age	$\text{RE}(\hat{v}_{15})$ in %age	$\text{RE}(\hat{m}_{100})$ in %age	$\text{RE}(\hat{v}_{100})$ in %age	1000 · KL
\tilde{Y}^E	-0.694 (-0.705)	4.425 (4.4002)	-0.0006 (0)	5.897 (5.882)	1.712
\tilde{Y}^M	-0.694 (-0.705)	5.602 (5.586)	-0.0006 (0)	7.092 (7.067)	0.449
\tilde{Y}^{L1}	-4.4404 (-4.4503)	0.8104 (0.786)	-4.917 (-4.917)	-0.191 (-0.216)	18.919
\tilde{Y}^{L2}	4.611 (4.601)	-1.163 (-1.187)	5.083 (5.083)	-0.191 (-0.216)	25.785
\tilde{Y}^{S1}	0.085 (0.075)	-0.1803 (-0.205)	0.083 (0.083)	-0.191 (-0.216)	0.012
\tilde{Y}^{S2}	-0.039 (-0.038)	0.228 (0.204)	-0.025 (-0.042)	0.281 (0.233)	0.018
$\Delta = 1$	$\text{RE}(\hat{m}_{15})$ in %age	$\text{RE}(\hat{v}_{15})$ in %age	$\text{RE}(\hat{m}_{100})$ in %age	$\text{RE}(\hat{v}_{100})$ in %age	1000 · KL
\tilde{Y}^E	-1.384 (-1.391)	9.315 (9.296)	0.006 (0)	12.461 (12.5)	6.3603
\tilde{Y}^M	-1.383 (-1.391)	11.796 (11.807)	0.003 (0)	14.957 (15.038)	2.002
\tilde{Y}^{L1}	-8.742 (-8.7499)	1.176 (1.169)	-9.663 (-9.667)	-0.921 (-0.862)	65.047
\tilde{Y}^{L2}	9.361 (9.353)	-2.762 (-2.769)	10.337 (10.333)	-0.921 (-0.862)	126.881
\tilde{Y}^{S1}	0.3097 (0.302)	-0.808 (-0.815)	0.337 (0.333)	-0.921 (-0.862)	0.262
\tilde{Y}^{S2}	-0.129 (-0.151)	0.9096 (0.814)	-0.164 (-0.166)	0.879 (0.928)	0.1598

5.2 Stationary distribution

As a further illustration, we investigate the stationary distribution of the IGBM. Under the conditions $\sigma^2\tau < 2$ and $\mu > 0$, the stationary distribution of Y exists and is an inverse gamma distribution [6, 18, 20, 52] with mean (5) and variance (6). The probability density function of the stationary distribution of Y , which we denote by f_{Y_∞} , is given by

$$f_{Y_\infty}(y; \alpha, \beta) := \frac{\beta^\alpha}{\Gamma(\alpha)} y^{-\alpha-1} e^{-\beta/y}, \quad (43)$$

where $\Gamma(\cdot)$ denotes the gamma function, $\alpha = 1 + 2/\sigma^2\tau$ and $\beta = 2\mu/\sigma^2$.

In Figure 6, we report the true stationary density f_{Y_∞} (43) (grey solid lines) and the densities \hat{f}_{Y_∞} , estimated from $n = 10^7$ simulated values of $Y(100)$, using the different numerical schemes. The densities are calculated with a kernel density estimator, i.e.,

$$f_{Y_\infty}(y) \approx \hat{f}_{Y_\infty}(y) := \frac{1}{nh} \sum_{k=1}^n \mathcal{K} \left(\frac{y - \tilde{Y}_k(100)}{h} \right),$$

where the bandwidth h is a smoothing parameter and \mathcal{K} is a kernel function (here Gaussian). If $\Delta = 0.5$ (left panel), the Strang splitting schemes accurately preserve the stationary density, while the other schemes yield estimates that deviate from the true density. This discrepancy increases as Δ increases (right panel), while the Strang schemes still yield satisfactory estimations. Hence, the Strang schemes do not only provide better estimations of the conditional and asymptotic moments (except for the asymptotic mean of the Euler-Maruyama and Milstein schemes if the condition $|1 - \Delta/\tau| < 1$ is satisfied), but also preserve the shape of the stationary density more accurately than the other numerical methods as Δ increases.

To quantify the distance between the true and the estimated densities under the considered numerical schemes for different time steps, we consider their Kullback-Leibler (KL) divergences given by

$$\text{KL} := \int f_{Y_\infty}(y) \log \left(\frac{f_{Y_\infty}(y)}{\hat{f}_{Y_\infty}(y)} \right) dy, \quad (44)$$

where the integral is approximated using trapezoidal integration. The results shown in Figure 6 are confirmed by the KL divergences (44) reported in Table 2. Similar results are obtained for other parameter configurations and choices of Δ . Note that, the Milstein scheme outperforms the Euler-Maruyama method in terms of preserving the shape of the stationary density, even though it introduces a larger bias in the asymptotic variance.

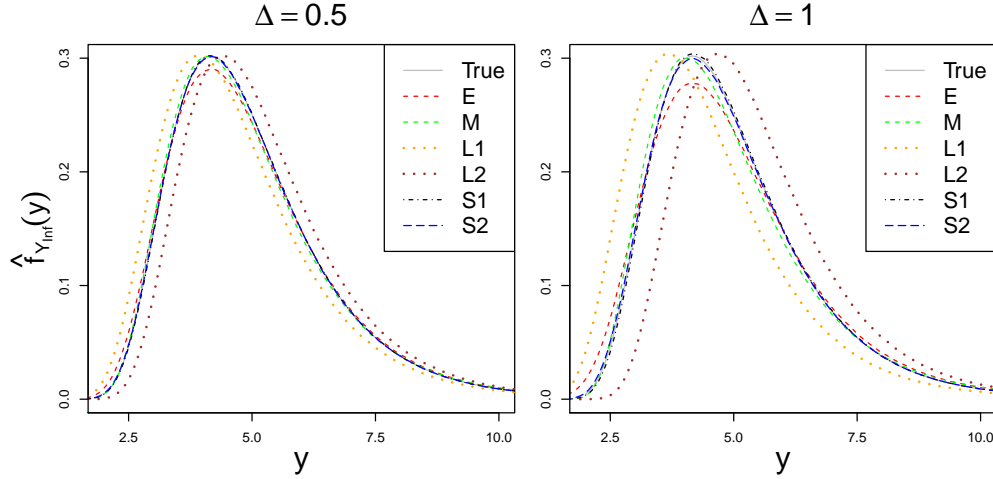


Figure 6: Comparison of the stationary density f_{Y_∞} (grey solid lines) and the estimated densities \hat{f}_{Y_∞} based on $n = 10^7$ simulations of $Y(100)$, generated with the different numerical schemes, for $\Delta = 0.5$ (left panel) and $\Delta = 1$ (right panel). The underlying parameters are $\mu = 1$, $\tau = 5$, $\sigma = 0.2$ and $Y_0 = 10$. The corresponding KL divergences (44) are reported in Table 2.

5.3 Boundary properties

An illustration of the preservation of the boundary properties by the splitting schemes is provided in Figure 7, where we report trajectories generated with the four splitting schemes when the boundary 0 is of entrance (top panel), unattainable and attracting (middle panel) and exit (bottom panel) type for $\mu = -0.5, 0$ and 0.5 , respectively, $\tau = 5$ and $\sigma = 1$.

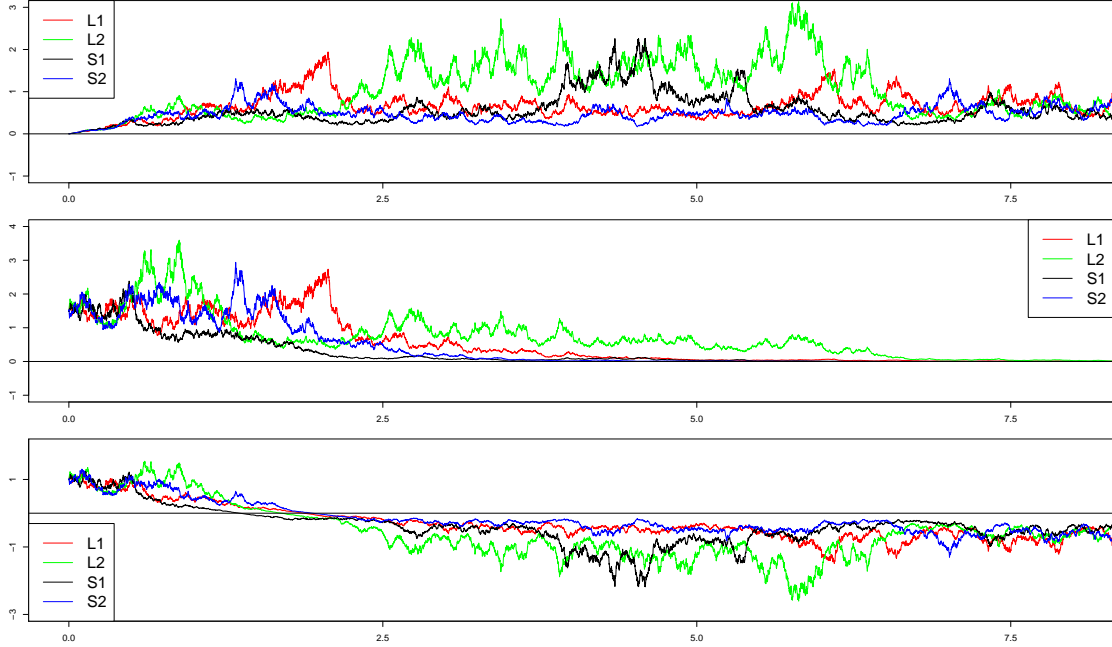


Figure 7: Trajectories of the IGBM generated with the different splitting schemes, for $\tau = 5$ and $\sigma = 1$. The parameter μ is chosen such that the boundary 0 is of entrance (top panel, $\mu = 0.5$), unattainable and attracting (middle panel, $\mu = 0$) and exit (bottom panel, $\mu = -0.5$) type.

5.4 Crossing probability

As a further illustration of the boundary behaviour, we investigate the probability that the process Y crosses the boundary 0 in a fixed time interval $(0, t_{\max}]$, with $t_{\max} > 0$ and $Y_0 > 0$. We define

$$T := \inf\{t > 0 : Y(t) \leq 0\} \quad (45)$$

as the first passage (hitting) time of Y through 0, and estimate the probability that $T < t_{\max}$ as follows

$$\mathbb{P}(T < t_{\max}) \approx \hat{F}_T(t_{\max}) := \frac{1}{n} \sum_{k=1}^n \mathbb{1}_{\{T_k < t_{\max}\}}, \quad (46)$$

where T_k denotes the crossing time (45), which is obtained from the k -th simulated path of Y and $\mathbb{1}_A$ denotes the indicator function of the set A . We are interested in situations where the process is in a high noisy regime, i.e., it is perturbed by a large noise intensity σ and is not in its stationary regime.

In Figure 8, we report $\mathbb{P}(T < t_{\max})$, estimated from $n = 10^6$ simulated trajectories under the different numerical schemes, as a function of μ , for $\sigma = 5$, $\tau = 5$, $Y_0 = 1$, $t_{\max} = 0.5$ and different choices of the time step, namely $\Delta = 0.01$ (left panel), $\Delta = 0.025$ (middle panel) and $\Delta = 0.05$ (right panel). The threshold 0 is of exit, unattainable and attracting (denoted by dashed grey vertical lines) or entrance type depending on whether $\mu < 0$, $\mu = 0$ or $\mu > 0$, respectively. When the boundary 0 is of entrance or unattainable and attracting type, it is known that $\mathbb{P}(T < t_{\max}) = 0$ for all values of t_{\max} . However, only the splitting schemes correctly preserve

this property, while the Euler-Maruyama method drastically fails for all considered values of Δ and the Milstein scheme only preserves it for small values of Δ (left and middle panels). The latter is in agreement with condition (40). Consider, e.g., $y = Y_0 = 1$. Then $\Delta < 5/122 \approx 0.0402$ and $\Delta < 5/127 \approx 0.0394$ is required in the entrance or unattainable and attracting case, respectively. In the exit scenario, the probabilities obtained from the Euler-Maruyama and Milstein schemes lie above those obtained from the splitting schemes. This suggests that the Euler-Maruyama and Milstein methods yield trajectories that exit from $[0, +\infty)$ faster than those generated from the splitting schemes. Similar results are obtained when studying these probabilities as a function of t_{\max} for fixed μ . Moreover, independent of the type of boundary behaviour, the crossing probabilities obtained from the splitting schemes seem not to vary significantly as Δ increases (a few undetected crossings may occur). This suggests their reliability even for large time steps, while those obtained from the Euler-Maruyama and Milstein schemes change for different choices of Δ .

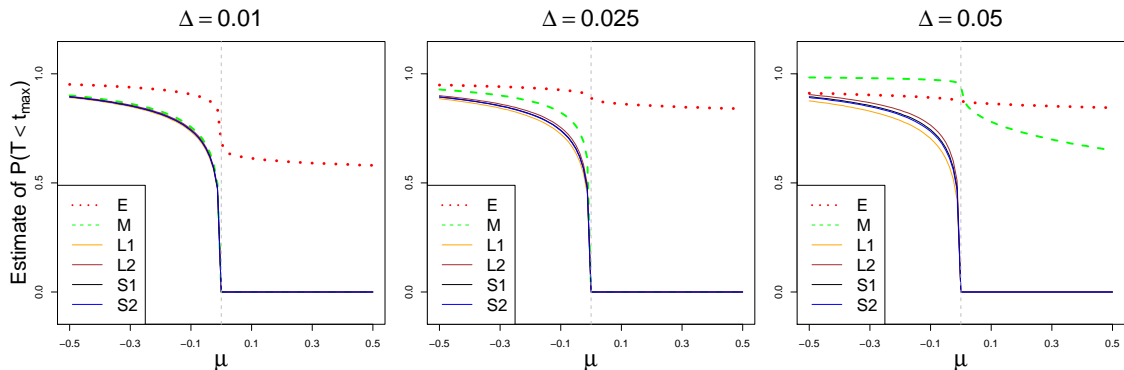


Figure 8: Probability $\mathbb{P}(T < t_{\max})$ (46), estimated from $n=10^6$ simulated trajectories under the different numerical schemes, as a function of μ , for different choices of the time step, namely $\Delta = 0.01$ (left panel), $\Delta = 0.025$ (middle panel) and $\Delta = 0.05$ (right panel), $t_{\max} = 0.5$, $\tau = \sigma = 5$ and $Y_0 = 1$. The boundary 0 is of entrance, unattainable and attracting or exit type depending on whether $\mu > 0$, $\mu = 0$ (denoted by dashed grey vertical lines) or $\mu < 0$, respectively.

6 Conclusion

Any numerical method, constructed to approximate a process of interest, should preserve its qualitative properties. Here, we focus on the IGBM, a process characterised by a constant inhomogeneous term, which can be considered as an extension of the well-studied GBM. We compare two Strang splitting schemes and two Lie-Trotter splitting schemes with the frequently applied Euler-Maruyama and Milstein methods both analytically and via simulations.

We provide closed-form expressions for the conditional and asymptotic means and variances of the considered numerical solutions, and analyse the resulting biases with respect to the true quantities. All splitting schemes yield better approximations of the variance of the process than the Euler-Maruyama and Milstein schemes. Moreover, in contrast to the frequently applied methods, the splitting schemes do not require extra conditions for the existence of the asymptotic quantities. Interestingly, the variances of the Lie-Trotter schemes and the first Strang scheme coincide asymptotically, while that of the second Strang scheme is different. If an extra condition, unrelated to the features of the model, is fulfilled, the Euler-Maruyama and Milstein schemes have an asymptotically unbiased mean. Overall, the Strang methods outperform both the Lie-Trotter schemes and the Euler-Maruyama and Milstein approximations in terms of preserving the conditional mean and variance of the process as well as its stationary density.

Moreover, in contrast to the frequently applied methods, all constructed splitting schemes preserve the different boundary properties of the IGBM, independently of the choice of the time discretisation step. We also investigate through simulations the probability that the process crosses the lower boundary. Compared to the splitting schemes, the Euler-Maruyama and Milstein methods suggest not only a positive crossing probability in the entrance or unattainable and attracting case, but also higher crossing probabilities in the exit scenario.

The closed-form expressions of the conditional and asymptotic means and variances allow for a direct control of the corresponding errors through the time discretisation step. One may argue that all methods perform comparably good for small enough stepsizes. However, there is a trade-off between computational time and quality of the simulation. To achieve a reasonable computation time, it may be necessary to avoid very small time steps. This becomes particularly important when the numerical method is embedded, e.g., in a simulation-based inference method [14, 51]. Moreover, even for arbitrary small time steps, there is no guarantee that the Euler-Maruyama and Milstein schemes would preserve the boundary properties, while the splitting schemes would still yield better approximations of the variance of the process. Finally, we note that the generation of one trajectory using the second Strang scheme requires twice as many random numbers as needed for the other methods, making the first Strang scheme, which performs comparably good throughout, the more computationally efficient choice.

The proposed test equation, its properties and their analysis are also meant as a contribution to extend the range of qualitative features that characterise the performance of numerical methods. The presented techniques may be extended to other numerical methods and SDEs, including multi-dimensional equations and processes with more general drift functions.

References

- [1] L.M. Abadie and J.M. Chamorro. Valuing flexibility: The case of an Integrated Gasification Combined Cycle power plant. *Energy Econ.*, 30(4):1850 – 1881, 2008.
- [2] M. Ableidinger and E. Buckwar. Splitting Integrators for the Stochastic Landau–Lifshitz Equation. *SIAM J. Sci. Comput.*, 38:A1788–A1806, 01 2016.
- [3] M. Ableidinger, E. Buckwar, and H. Hinterleitner. A Stochastic Version of the Jansen and Rit Neural Mass Model: Analysis and Numerics. *J. Math. Neurosci.*, 7(8), 2017.
- [4] A. Alfonsi. On the discretization schemes for the CIR (and Bessel squared) processes. *Monte Carlo Methods Appl.*, 11:355–384, 04 2005.
- [5] L. Arnold. *Stochastic differential equations: theory and applications*. Wiley, New York, 1974.
- [6] G. Barone-Adesi, H. Rasmussen, and C. Ravanelli. An option pricing formula for the GARCH diffusion model. *Comput. Stat. Data Anal.*, 49:287–310, 04 2005.
- [7] S. Blanes, F. Casas, and A. Murua. Splitting and composition methods in the numerical integration of differential equations. *Bol. Soc. Esp. Mat. Apl.*, 45, 01 2009.
- [8] C. E. Bréhier and Ludovic Goudenège. Analysis of Some Splitting Schemes for the Stochastic Allen-Cahn Equation. *Discrete Cont. Dyn.-B*, 24:4169–4190, 2019.
- [9] M. Brennan and E. S. Schwartz. A continuous time approach to the pricing of bonds. *J. Bank. Finance*, 3(2):133 – 155, 1979.
- [10] E. Buckwar and C. Kelly. Towards a Systematic Linear Stability Analysis of Numerical Methods for Systems of Stochastic Differential Equations. *SIAM J. Numer. Anal.*, 48(1):298–321, 01 2010.
- [11] E. Buckwar, M. G. Riedler, and P. E. Kloeden. The numerical stability of stochastic ordinary differential equations with additive noise. *Stoch. Dynam.*, 11(02n03):265–281, 2011.

- [12] E. Buckwar and T. Sickenberger. A comparative linear mean-square stability analysis of Maruyama- and Milstein-type methods. *Math. Comput. Simulat.*, 81(6):1110–1127, 2011.
- [13] E. Buckwar and T. Sickenberger. A structural analysis of asymptotic mean-square stability for multi-dimensional linear stochastic differential systems. *Appl. Numer. Math.*, 62(7):842–859, 2012.
- [14] E. Buckwar, M. Tamborrino, and I. Tubikanec. Spectral density-based and measure-preserving ABC for partially observed diffusion processes. An illustration on Hamiltonian SDEs. *Stat. Comput.*, 30(3):627–648, 2020.
- [15] K. C. Chan, G. A. Karolyi, F. A. Longstaff, and A. B. Sanders. An empirical comparison of alternative models of the short-term interest rate. *J. Finance*, 47(3):1209–1227, 1992.
- [16] J.C. Cox, J. Ingersoll, and S. Ross. A theory of the term structure of interest rates. *Econometrica*, 53(02):385–407, 1985.
- [17] S. Ditlevsen and P. Lansky. Estimation of the input parameters in the Feller neuronal model. *Phys. Rev. E*, 73:061910, 07 2006.
- [18] G. D’Onofrio, P. Lansky, and E. Pirozzi. On two diffusion neuronal models with multiplicative noise: The mean first-passage time properties. *Chaos*, 28:043103, 04 2018.
- [19] W. Feller. Two Singular Diffusion Problems. *Ann. Math.*, 54(1):173–182, 1951.
- [20] J. Forman and M. Sørensen. The Pearson diffusions: A class of statistically tractable diffusion processes. *Scand. J. Stat.*, 35(3):438–465, 2008.
- [21] E. Gobet. Euler schemes and half-space approximation for the simulation of diffusion in a domain. *ESAIM: PS*, 5:261–297, 2001.
- [22] R. Gutiérrez-Sánchez, L. M. Ricciardi, P. Román, and F. Torres-Ruiz. First-Passage-Time Densities for Time-Non-Homogeneous Diffusion Processes. *J. Appl. Probab.*, 34(3):623–631, 09 1997.
- [23] D. J. Higham. Mean-square and asymptotic stability of the stochastic theta method. *SIAM J. Numer. Anal.*, 38(3):753–769, 2000.
- [24] D. J. Higham and P. E. Kloeden. Numerical methods for nonlinear stochastic differential equations with jumps. *Numer. Math.*, 101(1):101–119, Jul 2005.
- [25] M. Insley. A Real Options Approach to the Valuation of a Forestry Investment. *J. Environ. Econ. Manage.*, 44(3):471 – 492, 2002.
- [26] C. Kahl, M. Günther, and T. Rossberg. Structure preserving stochastic integration schemes in interest rate derivative modeling. *Applied Numerical Mathematics*, 58(3):284 – 295, 2008.
- [27] S. Karlin and H. M Taylor. A second course in stochastic processes. *Academic Press, Vol. 2*, 1981.
- [28] R. Khasminskii. *Stochastic stability of differential equations*. Springer, 2., completely rev. and enl. ed. edition, 2011.
- [29] P. E. Kloeden and E. Platen. *Numerical Solution of Stochastic Differential Equations*. Springer, Berlin, 1992.
- [30] P. Lansky, L. Sacerdote, and F. Tomassetti. On the comparison of Feller and Ornstein-Uhlenbeck models for neural activity. *Biol. Cybern.*, 73:457–465, 11 1995.
- [31] B. Leimkuhler and C. Matthews. *Molecular dynamics: with deterministic and stochastic numerical methods*. Springer International Publ., Cham, 2015.

- [32] V. Linetsky. The spectral decomposition of the option value. *Int. J. of Theor. and Appl. Finance*, 07(03):337–384, 2004.
- [33] V. Mackevičius. On weak approximations of (a,b)-invariant diffusions. *Mathematics and Computers in Simulation*, 74(1):20 – 28, 2007.
- [34] S. J. A. Malham and A. Wiese. Stochastic Lie Group Integrators. *SIAM J. Sci. Comput.*, 30(2):597–617, 2008.
- [35] S. J. A. Malham and A. Wiese. Chi-square simulation of the CIR process and the Heston model. *Int. J. of Theor. Appl. Finance*, 16(03):1350014, 2013.
- [36] X. Mao. 3 - linear stochastic differential equations. In *Stochastic Differential Equations and Applications*, pages 91 – 106. Woodhead Publishing, second edition edition, 2011.
- [37] R. McLachlan and G. Quispel. Splitting methods. *Acta Numer.*, 11:341–434, 01 2002.
- [38] G. N. Milstein and M. V. Tretyakov. *Stochastic numerics for mathematical physics*. Scientific computation. Springer, Berlin, 2004.
- [39] G. Mircea. *Stochastic Systems. Uncertainty Quantification and Propagation*. Springer, London, 2012.
- [40] T. Misawa. A Lie Algebraic Approach to Numerical Integration of Stochastic Differential Equations. *SIAM J. Sci. Comput.*, 23(3):866–890, 2001.
- [41] E. Moro and H. Schurz. Boundary Preserving Semianalytic Numerical Algorithms for Stochastic Differential Equations. *SIAM J. Sci. Comput.*, 29:1525–1549, 01 2007.
- [42] W. P. Petersen. A General implicit splitting for stabilizing numerical simulations of Itô stochastic differential equations. *SIAM J. Numer. Anal.*, 35(4):1439–1451, 1998.
- [43] F. Pierret. A non-standard-Euler–Maruyama scheme. *Journal of Difference Equations and Applications*, 22(1):75–98, 2016.
- [44] Y. Saito and T. Mitsui. *T-stability of Numerical Scheme for Stochastic Differential Equations*, pages 333–344. World Sci. Ser. Appl. Anal., 1993.
- [45] Y. Saito and T. Mitsui. Stability Analysis of Numerical Schemes for Stochastic Differential Equations. *SIAM J. Numer. Anal.*, 33(6):2254–2267, 1996.
- [46] Y. Saito and T. Mitsui. Mean-square stability of numerical schemes for stochastic differential systems. *Vietnam J. Math.*, 30:551–560, 01 2002.
- [47] S. Sarkar. The effect of mean reversion on investment under uncertainty. *J. Econ. Dyn. Control*, 28(2):377 – 396, 2003.
- [48] T. Shardlow. Splitting for dissipative particle dynamics. *SIAM J. Sci. Comput.*, 24(4):1267–1282, 2003.
- [49] G. Strang. On the Construction and Comparison of Difference Schemes. *SIAM J. Numer. Anal.*, 5(3):506–517, 1968.
- [50] A. Tocino and M. J. Senosiain. Mean-square stability analysis of numerical schemes for stochastic differential systems. *J. Comput. Appl. Math.*, 236(10):2660–2672, 2012.
- [51] J. Voß. *An Introduction to Statistical Computing: A Simulation-based Approach*. Wiley series in computational statistics. Wiley, Chichester, West Sussex, 1. publ. edition, 2014.
- [52] B. Zhao. Inhomogeneous geometric Brownian motions. *SSRN Electron. J.*, 38, 2009.

A Proof of Proposition 1

Proof. Since the underlying X_j , $j = 1, \dots, k$, are iid, the mean and variance of W_k , $k \in \mathbb{N}$, are given by

$$\begin{aligned}\mathbb{E}[W_k] &= \mu_x^k, \\ \text{Var}(W_k) &= \text{Var}\left(\prod_{j=1}^k X_j\right) = \prod_{j=1}^k \mathbb{E}[X_j^2] - \prod_{j=1}^k \mathbb{E}[X_j]^2 = r^k - \mu_x^{2k}.\end{aligned}$$

Using the independence of W_k and H_{k+1} , the mean of Z_i conditioned on Z_0 is given by (23).

To compute the variance of Z_i conditioned on Z_0 , using the independence of W_k and H_{k+1} , we have that

$$\text{Var}(W_k H_{k+1}) = r^k r_h - \mu_x^{2k} \mu_h^2. \quad (47)$$

Further, we define $W_l^k := \prod_{j=l}^k X_j$, with $\mathbb{E}[W_l^k] = \mu_x^{k-l+1}$ and denote W_1^k by W_k . Using the fact that $W_j = W_k W_{k+1}^j$ for $k < j$ and that the underlying $X_j = M_j H_j$ are iid, the following relations for the covariance are obtained

$$\begin{aligned}\text{Cov}(W_j, W_k H_{k+1}) &\stackrel{k \leq j}{=} \text{Cov}(W_k W_{k+1}^j, W_k H_{k+1}) \\ &= \text{Cov}(W_k H_{k+1} M_{k+1} W_{k+2}^j, W_k H_{k+1}) \\ &= \text{Var}(W_k H_{k+1}) \mathbb{E}[M_{k+1} W_{k+2}^j] = [r^k r_h - \mu_x^{2k} \mu_h^2] \mu_m \mu_x^{j-k-1}, \quad (48) \\ \text{Cov}(W_j H_{j+1}, W_k H_{k+1}) &\stackrel{k \leq j}{=} \text{Cov}(W_k H_{k+1} M_{k+1} W_{k+2}^j H_{j+1}, W_k H_{k+1}) \\ &= \text{Var}(W_k H_{k+1}) \mathbb{E}[M_{k+1} W_{k+2}^j H_{j+1}] \\ &= [r^k r_h - \mu_x^{2k} \mu_h^2] \mu_m \mu_h \mu_x^{j-k-1}. \quad (49)\end{aligned}$$

Hence, the conditional variance of Z_i given Z_0 is given by

$$\begin{aligned}\text{Var}(Z_i | Z_0) &= Z_0^2 \text{Var}(W_i) + c_1^2 \text{Var}\left(\sum_{k=0}^I W_k H_{k+1}\right) + 2c_1 Z_0 \text{Cov}(W_i, \sum_{k=0}^I W_k H_{k+1}) \\ &= Z_0^2 \text{Var}(W_i) + c_1^2 \left[\sum_{k=0}^I \text{Var}(W_k H_{k+1}) + 2 \sum_{l=1}^I \sum_{k=0}^{l-1} \text{Cov}(W_l H_{l+1}, W_k W_{k+1}) \right] \\ &\quad + 2c_1 Z_0 \sum_{k=0}^I \text{Cov}(W_i, W_k H_{k+1}), \quad (50)\end{aligned}$$

yielding (24) after plugging (47), (48) and (49) into (50). \square

B Proof of Corollary 1

Proof. Since the Gaussian increments ξ_j entering in all numerical schemes are random variables with $\xi_j \sim \mathcal{N}(0, \Delta)$, the Euler-Maruyama scheme $\tilde{Y}^E(t_i)$ (16) can be rewritten as (22) with

$$X_j := \left(1 - \frac{\Delta}{\tau} + \sigma \xi_j\right) \sim \mathcal{N}\left(1 - \frac{\Delta}{\tau}, \sigma^2 \Delta\right),$$

$X_j = M_j$, $H_j = 1$ and the values reported in Table 1. Using the property that $\mathbb{E}[\xi_j] = \mathbb{E}[\xi_j^3] = 0$, $\mathbb{E}[\xi_j^2] = \Delta$, $\mathbb{E}[\xi_j^4] = 3\Delta^2$, the Milstein scheme $\tilde{Y}^M(t_i)$ (17) can be rewritten as (22) with

$$X_j := \left(1 - \frac{\Delta}{\tau} + \sigma \xi_j + (\xi_j^2 - \Delta) \frac{\sigma^2}{2}\right),$$

$X_j = M_j$, $H_j = 1$ and the values reported in Table 1.

The splitting scheme $\tilde{Y}^{L1}(t_i)$ (18) can be rewritten as (22) with

$$X_j := e^{-\left(\frac{1}{\tau} + \frac{\sigma^2}{2}\right)\Delta + \sigma \xi_j}, \quad (51)$$

$X_j = M_j$, $H_j = 1$ and the values reported in Table 1. Since $\xi_j \sim \mathcal{N}(0, \Delta)$, the random variable $-\left(1/\tau + \sigma^2/2\right)\Delta + \sigma \xi_j \sim \mathcal{N}\left(-\left(1/\tau + \sigma^2/2\right)\Delta, \sigma^2 \Delta\right)$, and thus the X_j , $j = 1, \dots, k$, are iid random variables with log-normal distribution, mean μ_x and second moment r given by

$$\begin{aligned} \mu_x = \mathbb{E}[X_j] &= e^{-\left(\frac{1}{\tau} + \frac{\sigma^2}{2}\right)\Delta + \frac{1}{2}\sigma^2 \Delta} = e^{-\Delta/\tau}, \\ r = \mathbb{E}[X_j^2] &= (e^{\sigma^2 \Delta} - 1)e^{-2\left(\frac{1}{\tau} + \frac{\sigma^2}{2}\right)\Delta + \sigma^2 \Delta} + e^{-2\Delta/\tau} = e^{\sigma^2 \Delta - 2\Delta/\tau}. \end{aligned}$$

Similarly, the splitting schemes $\tilde{Y}^{L2}(t_i)$ (19) and $\tilde{Y}^{S1}(t_i)$ (20) can be rewritten as (22) with X_j given by (51), as for \tilde{Y}^{L1} , and the values reported in Table 1. Further, since φ_j and ψ_j are iid random variables distributed as $\mathcal{N}(0, \Delta/2)$, we have that $\xi_j := \varphi_j + \psi_j \sim \mathcal{N}(0, \Delta)$. Setting

$$H_j := e^{-\left(\frac{1}{\tau} + \frac{\sigma^2}{2}\right)\frac{\Delta}{2} + \sigma \psi_j}, \quad M_j := e^{-\left(\frac{1}{\tau} + \frac{\sigma^2}{2}\right)\frac{\Delta}{2} + \sigma \varphi_j},$$

the splitting scheme $\tilde{Y}^{S2}(t_i)$ (21) can be rewritten as (22) with the values reported in Table 1. \square

C Proof of Proposition 2

Proof. When letting $i \rightarrow \infty$ (and thus $I \rightarrow \infty$), $\sum_{k=1}^I \mu_x^k$ converges to $\mu_x/(1 - \mu_x)$ if and only if $|\mu_x| < 1$. Under the same condition, $\mu_x^i \rightarrow 0$, yielding the asymptotic mean of Z_i given by (27).

Letting $i \rightarrow \infty$ (and thus $I \rightarrow \infty$), $\sum_{k=1}^I (r^k r_h - \mu_x^{2k} \mu_h^2)$ converges if and only if $r \in (0, 1)$ and $|\mu_x| < 1$. Hence, under these conditions,

$$\begin{aligned} \lim_{i \rightarrow \infty} Z_0^2(r^i - \mu_x^{2i}) &= 0, \\ \lim_{i \rightarrow \infty} \sum_{k=0}^I r^k r_h - \mu_x^{2k} \mu_h^2 &= -\frac{r_h}{r-1} + \frac{\mu_h^2}{(\mu_x^2 - 1)}, \\ \lim_{i \rightarrow \infty} \sum_{l=1}^I \sum_{k=0}^{l-1} [r^k r_h - \mu_x^{2k} \mu_h^2] \mu_m \mu_h \mu_x^{l-k-1} &= -\frac{\mu_m(r_h \mu_h - \mu_h^3 - r_h \mu_h \mu_x^2 + \mu_h^3 r)}{(\mu_x - 1)^2(1 + \mu_x)(r-1)}, \\ \lim_{i \rightarrow \infty} \sum_{k=1}^I [r^k r_h - \mu_x^{2k} \mu_h^2] \mu_m \mu_x^{i-k-1} &= 0, \end{aligned}$$

leading to the asymptotic variance of Z_i given by (28). \square